REACTIVE HOT PRESSING OF BOEHMITE ($\alpha Al_2O_3 \cdot H_2O$)

BY

ROSS STANLEY BRADBEER

B.Sc., University of British Columbia, 1965

A THESIS SUBMITTED IN PARTIAL FULFILMENT OF

THE REQUIREMENTS FOR THE DEGREE OF

MASTER OF SCIENCE

in the Department

of

METALLURGY

We accept this thesis as conforming to the

required standard

THE UNIVERSITY OF BRITISH COLUMBIA

January, 1972

In presenting this thesis in partial fulfilment of the requirements for an advanced degree at the University of British Columbia, I agree that the Library shall make it freely available for reference and study. I further agree that permission for extensive copying of this thesis for scholarly purposes may be granted by the Head of my Department or by his representatives. It is understood that copying or publication of this thesis for financial gain shall not be allowed without my written permission.

Department of Metallurgy

The University of British Columbia
Vancouver 8, Canada

Date February 9, 1972

ABSTRACT

The compaction behaviour of boehmite has been studied under isothermal conditions,with special emphasis devoted to hot pressing in the temperature range 300 to 600°C.

The present work indicates that it is possible to produce a hard dense compact under certain conditions. However, the behaviour of the material during reactive hot pressing appears to be more complicated than can be explained by simple sintering or kinetic theories.

To aid in understanding the mechanisms of compaction during a phase transformation, the behaviour of the system during reactive hot pressing was studied from a purely phenomenological point of view, a viscoelastic model. By using viscoelastic theory it is possible to relate ideal elastic and energy-absorbing or damping viscous parameters to the behaviour of boehmite during R.H.P.

While the apparent compact density varied as a complex function of temperature, it was found that the overall compaction behaviour of boehmite could be adequately described by a second order linear differential equation, which in turn could be related to a combination of elastic (displacement sensitive) and viscous (strain rate sensitive) components.

The viscous nature of the powder during R.H.P. reached a maximum value just before the boehmite to gamma transition (380 to 443°C), suggesting that strong particle interaction was occurring.

It is anticipated that R.H.P. from 380 to 443°C will lead to the most favourable particle rearrangement for producing a hard gamma phase at 500°C.

In producing the "hard phase" it was important to maintain a critical water concentration. Approximately 4% retained water was necessary for forming a hard dense compact. On the other hand in the presence of an excessive water vapor pressure, the unreacted boehmite powder appeared to transform directly to alpha alumina, resulting in a friable compact. Thus the need for maintaining the correct vapor pressure during R.H.P. is essential.

Production of the "hard phase" material at 500°C appears promising as an intermediate step in producing strong translucent bodies upon subsequent sintering at 1000°C.

ACKNOWLEDGEMENTS

The author wishes to express his gratitude for the advice and encouragement of his research supervisor, Dr. A.C.D. Chaklader. Thanks are also extended to faculty members, fellow graduate students, and technical staff, especially Professor R.G. Butters for helpful discussions and assistance. Financial assistance from the Defence Research Board, grant #7565-07 is gratefully acknowledged.

TABLE OF CONTENTS

LIST OF FIGURES

LIST OF TABLES

1. INTRODUCTION

1.1 Alumina

Alumina is the most commonly used oxide ceramic. This is not surprising in view of the fact compounds of aluminum are abundant on the Earth's crust. Because of its availability, high melting temperature (2035°C) and chemical inertness, alumina has been used in an ever increasing number of products.

In addition to its conventional usage such as in refractories, crucibles, furnace tubes etc., it has been extensively used in a great number of electronic applications. The ability to retain high electrical resistance (10^{14} ohm-cm at room temperature) at increasingly high temperatures and voltages, its excellent dielectric strength, and low dielectric loss, have made alumina a very good insulator. Among the new ceramic insulators made of alumina are spacers used in vacuum tubes, substrate bases for thin film integrated and hybrid circuits.

Because of its wide and diversified applications a large number of fabrication techniques are employed to shape and process alumina products. Although cold pressing and subsequent sintering at temperatures above 1600°C is the most conventional; slip casting, extrusion, and rolling using an organic binder, are also extensively used for specialized products.

These traditional methods of forming suffer from the limitation that the parts must be dried for long periods before final sintering. Furthermore, during drying and firing, up to 25-30% volume shrinkage will occur which unless carefully controlled may produce warpage and cracking in the products.

Other techniques which have been used for fabricating alumina products during final firing are isostatic pressing, hot pressing, hot extrusion and hot-forging (1). However, none of these high temperature processes have been extensively used commercially because of the limitations of die materials, and high temperatures involved in these processes. On the other hand, these high temperature processes have the capability of fabricating very high density products with close dimensional tolerance. Generally, these are relatively expensive items.

Reactive hot pressing is a low temperature hot pressing process, which has recently been investigated by several workers (2) and which has the potential of becoming a commercial process. Reactive hot pressing is essentially a hot pressing technique which is carried out in conjunction with either a decomposition or a polymorphic reaction. Hot pressing of a number of oxides compositions has been given particular attention in recent years with respect to achieving dense fine grained microstructure. With the trend towards finer-grain ceramics, not only have new ultrafine materials been developed but efforts have been directed towards starting with ultrafine materials which have a different crystal structure from that of the final hot-pressed product. This is one of the main reasons for interest in reactive hot pressing for fabricating ceramic products. It has been suggested that the

application of pressure during a phase transformation or a decomposition reaction can produce considerable interparticle bonding, resulting in the formation of a strong and dense body. In producing translucent dense alumina products for use in high pressure sodium vapor lamps, Bates (3) used boehmite as the precursor material and was able to produce fully dense translucent alumina by first prefiring the material at 400°C then sintering at 1725°C for five hours. Bates used three different types of boehmite, boehmite "A", which has small crystallite size of 100 Å; boehmite "B", fibrillar material of particle dimension 50 Å by 1000 Å; and boehmite "C", which had large grain size (1-5 μ). In contrast to boehmite "A" and "B", boehmite "C" decomposed to alpha alumina directly at 500°C. On the other hand, dense translucent gamma alumina can be produced by reactive hot pressing fibrillar boehmite at 500°C under 8000 psi.

1.2 Previous Work

MacKenzie[22] was the first worker to hot press boehmite in the temperature range 300 to 600°C. He observed enhanced compaction when boehmite was reactive hot pressed during the decomposition reaction (boehmite to gamma alumina) at 500°C. Cook and Chaklader (4) suggested that the degree of compaction should be proportional to the weight loss due to dehydroxylation. However, their results were inconclusive, indicating that the true mechanism or mechanisms of compaction could not be determined solely by weight loss studies. To explain densification in the presence of an applied stress, they suggested that large scale particle rearrangement must exist. They concluded

that fragmentation during the dehydroxylation process may significantly affect the particle flow. Likewise, equally important mechanisms would be (i) particle sliding and (ii) elastic and plastic deformation.

St-Jacques (5) investigated under vacuum, the flow behaviour of cold compacted cylindrical specimens of fibrillar colloidal boehmite by compression creep tests. He suggested that the creep rate was proportional to the applied stress between 350 and 550°C and 31 to 265 psi. By assuming that the same packing geometry was retained during the reaction and that shrinkage was due only to neck growth, St-Jacques derived a simple relationship to express the change of length of the compact with time. The equation had the form $\frac{\Delta L}{L_o} = Kt^{n/4}$ where $\frac{\Delta L}{L_o}$ is the strain, "K" and "n" are constants and "t" is the time. A log-log plot of his data produced a straight line only over a limited interval of time. From the slope, "n" was found to be approximately equal to 5, which according to sintering theory indicated that neck growth was due to the volume diffusion mechanism. One disadvantage of St-Jacques simple approach was that "K" was found to be a function of temperature and pressure. This alone would suggest the problem was far more complex than indicated by his analysis. Moreover, the conclusion that "sintering is due to a volume diffusion mechanism" is not justified and requires further study for confirmation.

1.3 Objectives of the Present Study

The objective of this work is to extend the study of reactive hot pressing of boehmite, with special emphasis on hot pressing in the temperature range 300° to 600°C. It has been indicated that the

behaviour of boehmite during reactive hot pressing is much more complicated than that suggested by previous workers. For this reason, no effort has been made to use sintering or kinetic theories to study the compaction behaviour of boehmite. Instead a more empirical approach, a viscoelastic model" was used to interpret the data.

This approach allows one to express the behaviour of boehmite during R.H.P. in terms of ideal elastic and viscous components. By plotting these components as a function of temperature it should be possible to correlate the behaviour of boehmite during R.H.P. to data obtained from X-ray, T.G.A., D.T.A. and electron microscope analyses. Since a phase transformation is involved during reactive hot pressing operations, it will be informative to include the transformation sequences for hydrates of alumina, which on heating in air convert to alpha alumina directly or indirectly. This is shown in Figure 1.

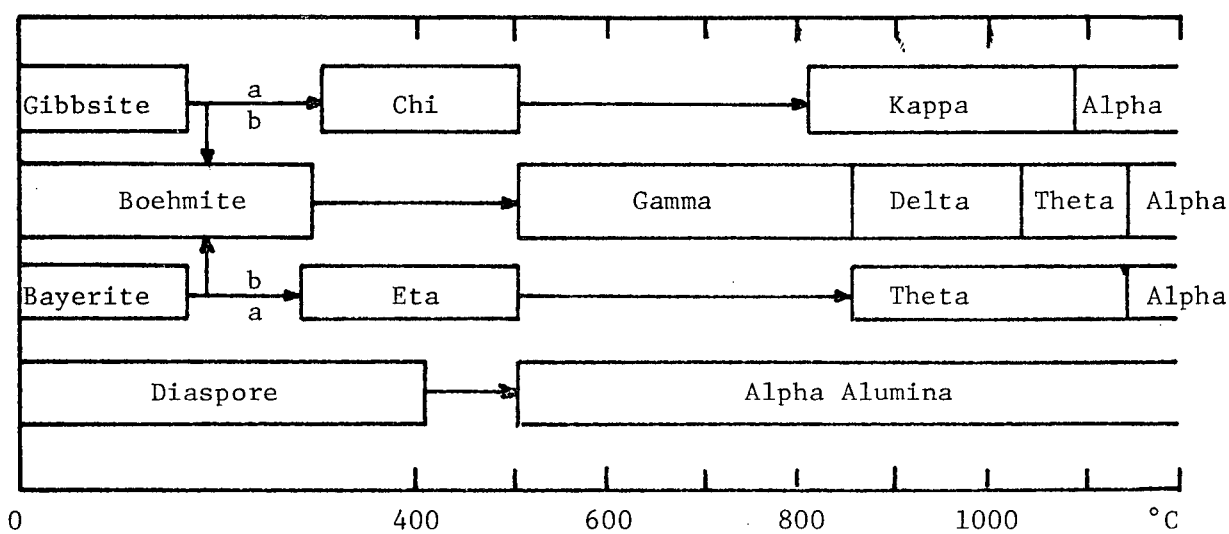

Figure 1. Dehydration sequence of alumina hydrates in air.

Note: Path "b" is favored by moisture, alkalinity, and coarse particle size (100 micron); path "a" by fine crystal size (below 10 microns).

The above sequences of transitions (Figure 1), is mainly due to Strumph et al. and Terian and Papee (6), and is generally accepted, although there is controversy about the X-ray identification of some phases and the existence of others. The sequences are affected not only by the starting materials but also by their degree of crystallinity, heating rates, and impurities.

Two important transitions, relevant to this study are the boehmite transition and the diaspore transition.

Boehmite transition ($\alpha Al_2O_3.H_2O$)

Coarse hydrothermal boehmite (surface area less than 15 m^2/g) prepared from gelatinous aluminum hydroxide, gibbsite, bayerite or higher transition phases, by digestion in H_2O at temperatures above 150°C, transforms to gamma (360 to 860°C), to delta, to theta, and finally to alpha alumina, on heating progressively at higher and higher temperatures.

Fibrillar colloidal boehmite on the other hand, transforms to gamma at 500°C, to theta at 1000°C, and to alpha alumina at 1200°C.

Diaspore transition ($\beta Al_2O_3.H_2O$)

Deflandre (7) in 1932 showed that diaspore transforms directly to corundum (alpha alumina) by an ordering process and without intermediate products, at about 450 to 600°C.

For this reason, when reactive hot pressing boehmite the following factors must be considered.

(i) Does the precursor material undergo one or more phase transformations in the temperature range used for R.H.P.?

(ii) What is the nature of the transformation involved? Does it depend upon the presence of water etc? If so, what is the effect of vapor pressure? The vapor pressure could increase or decrease the phase transformation temperature (Clapeyron equation). Secondly, a precursor material that undergoes a transformation sequence, for example, a → b → c as the temperature is increased, could in the presence of a high pressure environment, transform directly from phase "a" to phase "c". Under these conditions phase "b" would not appear.

2. EXPERIMENTAL

2.1 Material

The material used in this study was colloidal boehmite supplied by E.I. du Pont De Nemours and company under its trademark name of "Baymal". The characteristics of the powder are described by Iler (8) as having AlOOH, 83.1%; physically adsorbed water, 1.8%; chemically bound water, 3.3%; sulphate as $SO_4^=$, 1.75%. The true density of the material is 2.28 grams per cc. The particles are fibrillar, being about 50 Å in diameter and 1000 to 2000 Å long.

Boehmite on heating from room temperature to 1200°C undergoes two distinct and well known phase transformations, boehmite to gamma alumina at 480°C and gamma to alpha alumina at 1200°C. It is possible that the latter transition temperature may be affected by the presence of water vapor pressure in the system. The dehydroxylation of boehmite to gamma alumina involves only a minor change in the overall structure. Boehmite is believed to be of orthorhombic symmetry (9). The structure consists of oxygen ion layers within which the oxygen ions are cubic packed, while hydroxyl ions are situated between these layers to form zig-zag chains. Molecular water is not present (10) in boehmite, however, because of its large surface area (250 m^2/gm) it tends to pick up a measurable amount of water over the formula $Al_2O_3.H_2O$ as physically adsorbed water.

Gamma alumina has a cubic structure. It has been concluded (11) that the dehydroxylation scheme of boehmite is based on the cubic oxygen layer sequence ABC,ABC..., which is found in gamma alumina. Although the formula for gamma alumina is usually written as γ-Al_2O_3, Glemser and Rieck observed that all gamma alumina has water strongly bound as hydroxyl ions, i.e., γ-$Al_2O_3.xH_2O$, where $x << 1$.

2.2 Reactive Hot Pressing of Boehmite (R.H.P.)

For a detailed study of the hot pressing characteristics of boehmite three different techniques were used:

(a) Reactive hot pressing of boehmite was carried out isothermally at different temperatures, in each case the pressure was maintained constant at 5860 psi. A steel die was used in which only one ram was moveable. The clearance between the rams and die wall was sufficient to allow the gas phase produced during decomposition to escape. For heating, a Philips 12 KW induction unit generator was used. The die itself acted as the susceptor.

Ideally one would like to start with a loose powder. However, this was impractical for the following reasons. Loosely packed boehmite powder compacts reduce in the ratio 8:1 when cold pressed to a green density of approximately 1.5 gm/cc (0.60 relative density). Thus to produce a 0.5 inch compact approximately 4.0 inches ram displacement would be required. Although it is possible to measure accurately such a large displacement, due to the fine particle size of boehmite, the loose powder tends to jam between the ram and die wall, resulting in exceedingly high ram-die friction. To avoid this problem weighed amounts of boehmite powder were precompacted at 2000 psi. The ram was

was then removed and any excess powder trapped between the die wall and rams was scrapped off. The die assembly containing the powder was then placed in the induction furnace, and further pressed at 5860 psi. After mechanical equilibrium had been attained the pressure was lowered to 600 psi. The powder was then heated to the desired temperature. After waiting ten to fifteen minutes, to ensure temperature equilibrium was established, the dial guage reading was noted. This value being recorded as the initial compact length "L_o". The pressure was then increased to 5860 psi and the change in compaction was recorded as a function of time. The pressure was then released, the specimen after being cooled to room temperature, was removed from the die. The final dimensions were then recorded from which the "end point density" could be calculated. Figure 2 shows a diagram of the apparatus and a schematic representation of a typical R.H.P. cycle. This configuration was used only to study the compaction behaviour of boehmite.

(b) In a second set of experiments a steel die with floating rams was used (Figure 3-A). To facilitate easy removal of the compact after R.H.P. a graphite sleeve was inserted between the rams and die. Graphite discs were placed between the compact and the rams. The presence of the graphite sleeve, besides facilitating easy removal of the compact after R.H.P. inhibited or restricted the escape of water vapor. More important, it appeared that a hard crystalline compact could be produced at temperatures less than 700°C only when a graphite sleeve was used. Figure 4 shows a compact which was R.H.P. at 700°C and 8000 psi. However, the use of a graphite sleeve had two disadvantages; (i) It produced non-uniform specimens. Usually only part of the compact

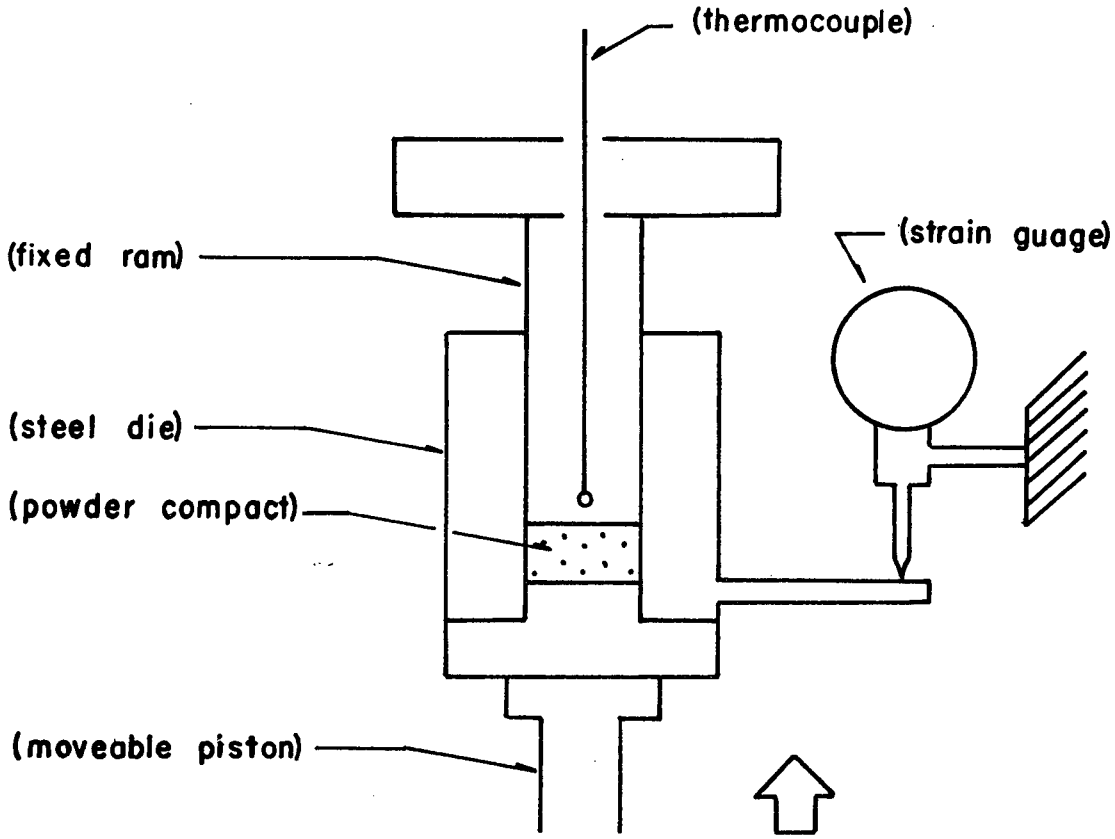

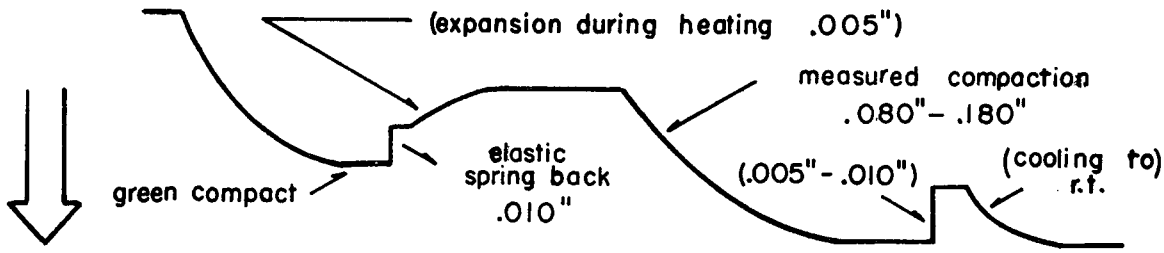

compaction profile

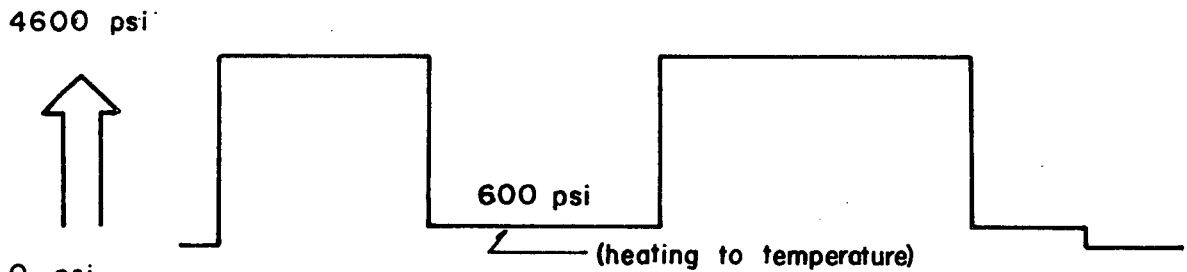

applied pressure

Figure 2. Diagram of compaction apparatus and a schematic representation of a typical R.H.P. cycle.

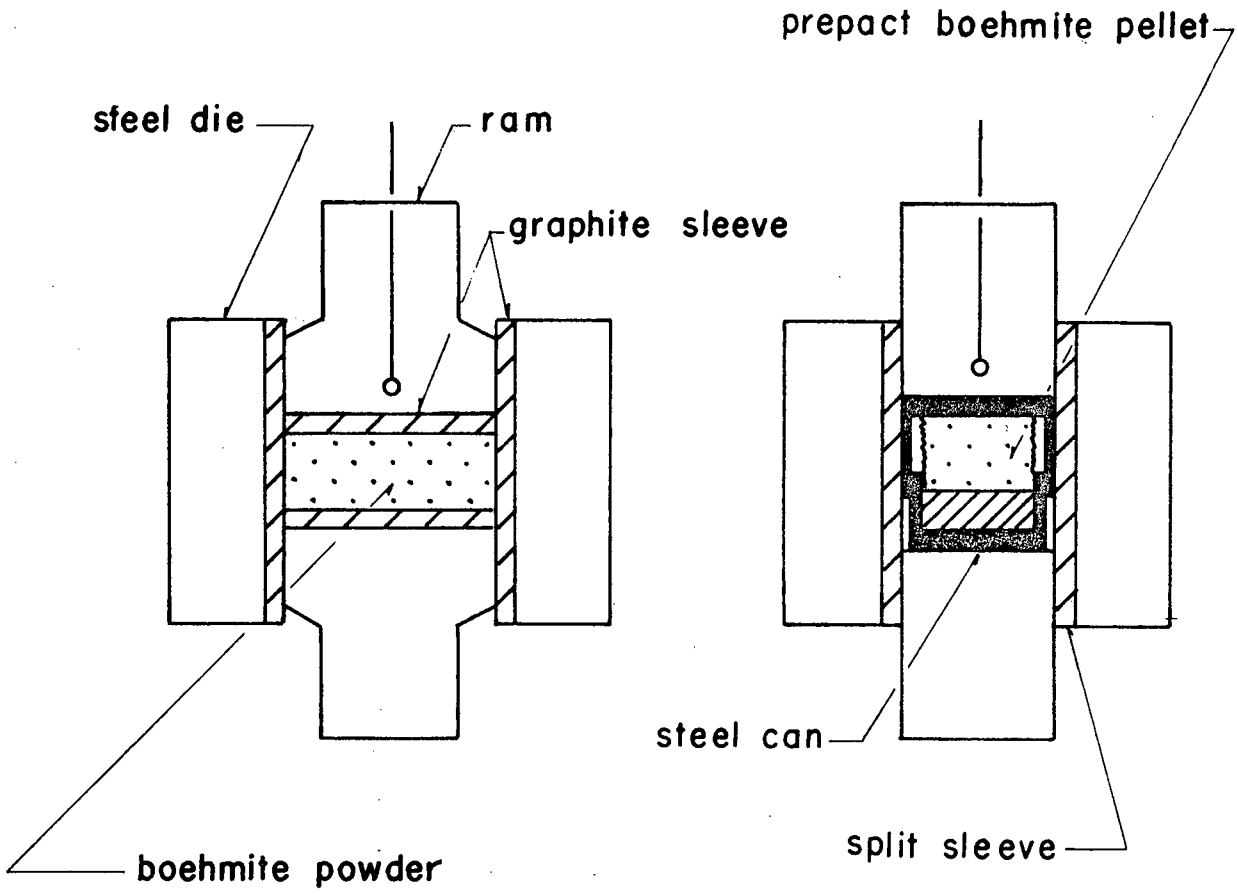

Figure 3. A - R.H.P. using a graphite sleeve

B - Configuration used for "canning".

The die assembly was heated by induction heating.

was converted to a dense "hard phase", and (ii) Reproducibility of the results was generally poor. In many cases the "hard phase" material could not be reproduced, even under the same experimental conditions.

(c) In an attempt to obtain a more uniform product, precompacted boehmite pellets (50% green density) were completely encapsulated or canned. The configuration for canning is shown in Figure (3-B). R.H.P. experiments for both the canning operation and hot pressing using a graphite sleeve were repeated for temperatures ranging between room temperature and 700°C and pressures ranging from 4,000 to 20,000 psi.

2.3 Water Loss Versus Hardness

To determine if there may be a correlation between the hardness of the material obtained during R.H.P. and retained water, water loss versus hardness experiments were performed. First, the hardness at indicated locations on specimen 1 (see Figure 4), was measured using a Tukon Tester (136 DPH) microhardness machine. Then samples (5 mg) were scraped from the corresponding locations and placed in a Dupont 950 Thermogravimetric Analyzer. The change in weight due to water loss was then measured upon heating each sample to 600°C.

2.4 Electron Microscope Studies

To observe how boehmite behaves during heat treatment, Dupont Baymal Colloidal alumina (boehmite) was first heated to 600°C for 24 hours, then placed in a Hitachi HU-11A electron microscope. Both electron transmission and diffraction photographs were taken. The very fine particles were mounted on a carbon support film by suspending the powder in alcohol, then the alcohol was allowed to evaporate, leaving

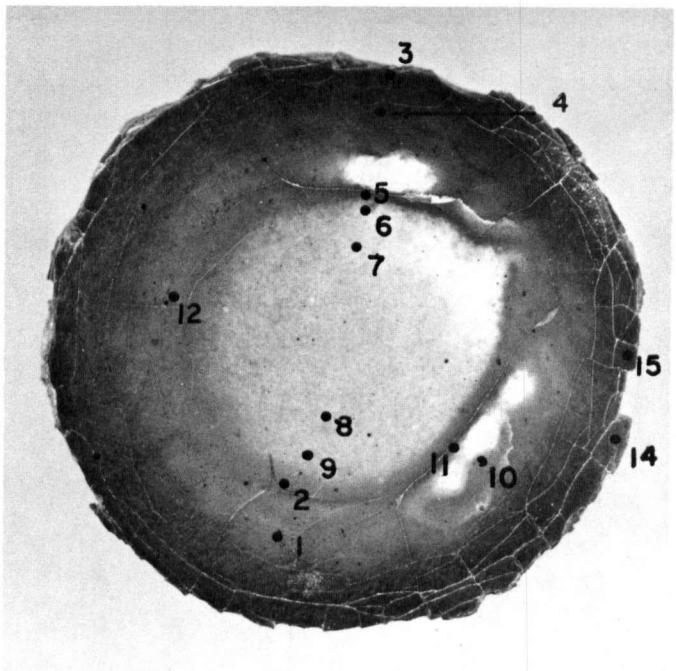

"A". Numerals indicate locations from which water loss and hardness measurements were taken.

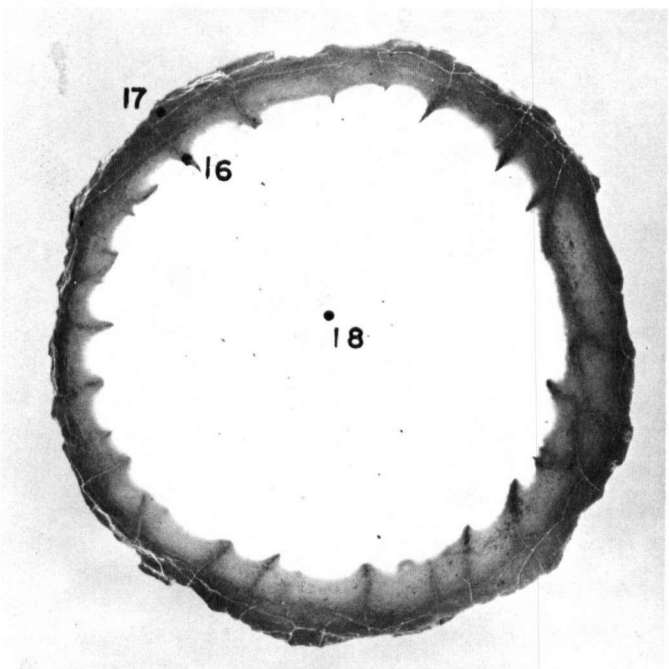

Figure 4. Boehmite compact R.H.P. at 700°C and 8000 psi (using graphite sleeve). Figures A and B show the top and bottom of specimen 1.

the particles deposited on the film. The diffraction patterns were obtained. The camera constant was determined using a gold film. The "d spacing" can be calculated from the powder patterns using

$$d = \frac{\text{camera constant}}{R}$$

where "R" is the distance from the center of the diffraction pattern to a diffraction spot or a ring.

2.5 X-Ray Studies

X-ray studies on powder specimens were carried out using a Norelco X-ray diffractometer. When only small quantities of material were available, Debye-Scherrer cameras of the Buerger design were used. All diffraction patterns were taken using the copper K_α radiation.

In addition to identification of the powder pattern using the A.S.T.M. diffraction data file, line broadening techniques were used to determine crystallite size. For this purpose, the method detailed in Klug and Alexander (12) was used. In each case, the diffraction peak to be studied was scanned at the rate of 1/4° per minute using the maximum time constant. Both the source and receiver slits were 1°. "B" the total line broadening due to both instrument broadening "b" and crystallite size were obtained by measuring the angular width at half maximum intensity. Instrument line broadening was determined by using a silicon standard for which the grain size was greater than 1000 Å.

3. RESULTS

3.1 Reactive Hot Pressing "Graphite Sleeve" Versus "Canning"

As previously discussed, if a graphite sleeve was used during R.H.P., it was possible to produce a very hard, apparently non-porous phase (apparent density 2.2 gm/cc). The bulk of this phase was generally limited to the outer edges of the specimen (Figure 4).

The "hard phase" exhibited the following properties; (i) thin sections of the material were translucent while thicker sections appeared black, (ii) the material was brittle and fractured easily, and (iii) the material showed a pronounced preferential cracking, in that it contained a large number of vertical cracks whose fracture planes ran parallel to the stress axis.

After a number of unsuccessful attempts to produce a uniform product using a graphite sleeve, pellets of boehmite powder were pre-compacted to 50% green density, "canned" and then hot pressed at various temperatures and pressures. The results can be summarized as follows:

(i) Due to "canning" too much water was retained, and as a result, the final compact was a wet friable powder. To eliminate this problem the powder was first calcined at various temperatures to remove part

of the structural water. The powder was then "canned" and R.H.P. as before.

(ii) Generally, because of the calcining operation too much water was lost. This resulted in a very poor friable white compact. It was possible only once to retain the correct amount of water, the product in this case was black in appearance and very brittle. Unfortunately, it was also highly fractured due to incomplete compaction which was a result of the "canning" prodedure used during hot pressing. While "canning" looked optimistic, the operation was given up in favor of other studies.

3.2 Water Loss Versus Hardness

It is apparent from the preceding section that there may be a definite correlation between hardness and retained water. Therefore, hardness and water loss studies were made on specimen 1 (Figure 4) at the indicated locations. The results are summarized in Table I and Figure 5,which is a plot of hardness versus percent retained water.

(i) The soft white material contained less than 1% retained water (point 18, Figure 4-B).

(ii) The "hard phase" material contained from 4% to 5% retained water (point 3, Figure 4-A).

Although no exact correlation between retained water and hardness could be determined, the microhardness of the material increased as one approached a fracture surface. For example, at point 16, Figure 4-B, a fracture surface is running from the edge to the center of the specimen. The material at the edges of the fracture surface exhibited the maximum hardness observed (400 DPH).

Point	Average hardness DPH 136°	Retained water %	X-ray structure	Crystallite size
1	340	7.2		
2	390	-		
3	390	3.6		
4	390	5.5		
5	360	-		
6	260	-		
7	120	-		
8	200	1.4		
9	210	-		
10	290	-		
11	340	-		
12	420	3.5		
14	420	-	gamma alumina	53 Å dia
15	270	10.7		
16	400	-		
17	290	-		
18	0	0.7	alpha alumina	1.0 μ
Edge	-	-	gamma alumina	

* Soft white material (hardness could not be measured, assumed equal to zero).

Table I. Hardness versus retained water for the indicated locations on specimen 1.

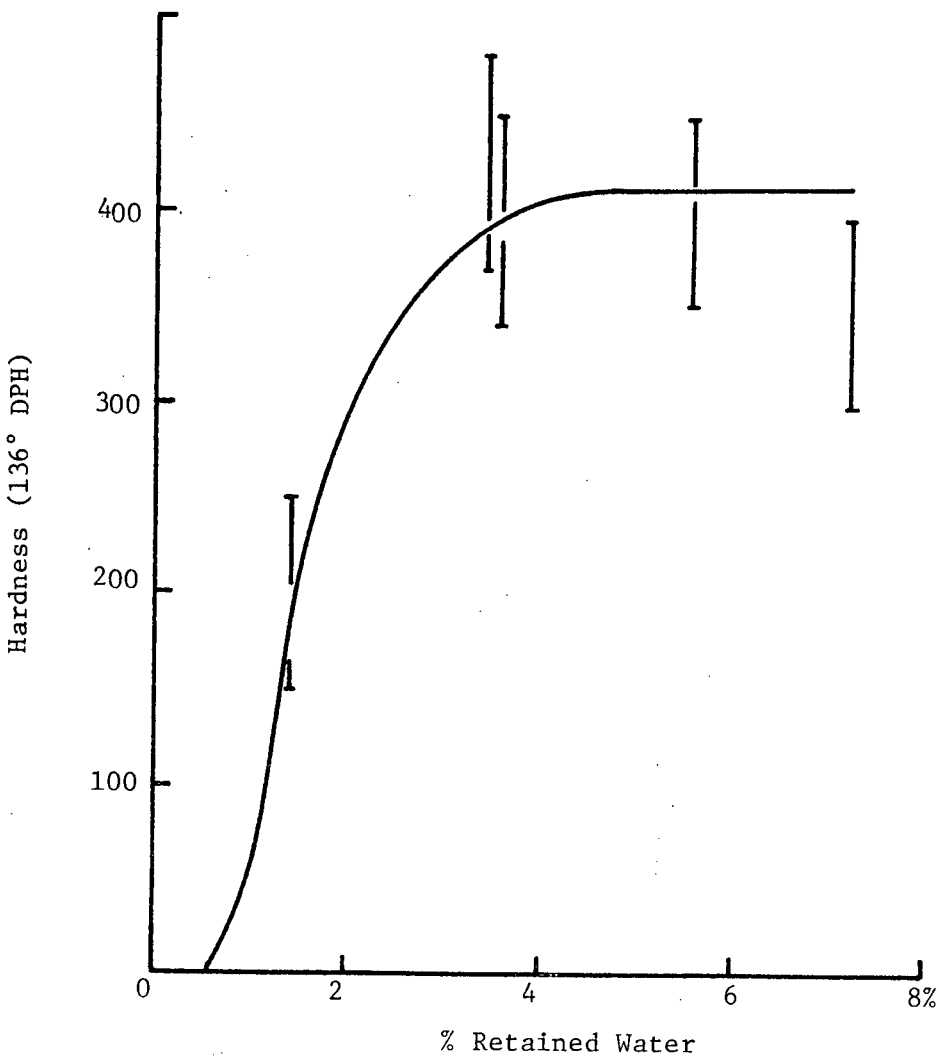

Figure 5. Hardness versus retained water.

3.3 X-Ray Analysis

From X-ray analyses of specimen 1 (Figure 4) the following results were obtained:

Point 18 - the soft white material was alpha alumina.

Point 14 - material taken from point 14 was gamma alumina. Similarly samples taken from the edge of specimen 1 were gamma alumina.

Because of the method of heating the specimen (induction heating, the die acted as the susceptor and the rams as the heat sink) the outer edges would be hotter than the center region. Thus alpha alumina should be formed near the edges and gamma alumina in the central region, just opposite to what was observed.

In order to explain the anomalous behaviour, further studies were made by heat treating boehmite at different temperatures. Boehmite powder was heat treated (one atmosphere) at the following temperatures for 24 hours and the phases were identified by X-ray diffraction techniques. The results are as follows:

Boehmite heated to	400°C	for 24 hours	boehmite
"	500°C	"	gamma alumina
"	600°C	"	gamma alumina
"	750°C	"	gamma alumina

Iler (8) obtained exactly the same results in a similar study with fibrillar boehmite. The X-ray diffractometer curves of heat treated boehmite as obtained by Iler are shown in Figure 6. It is noted that at atmospheric pressure boehmite is not converted to alpha alumina until 1200°C. A small sample of boehmite which had been heat treated at 600°C (gamma alumina) was examined under the electron microscope. In the

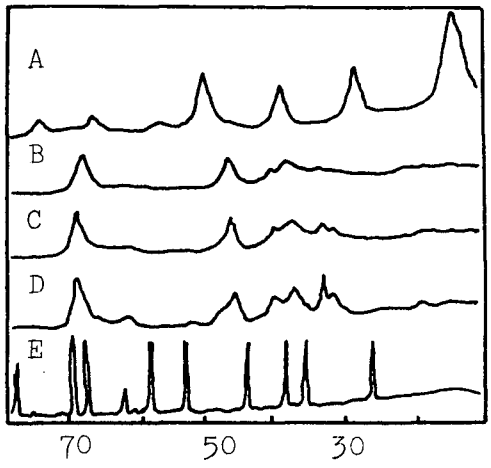

Figure 6. X-Ray diffraction curves of aluminas from fibrillar colloidal boehmite. (A) colloidal boehmite, (B) gamma (700°C), (C) gamma (900°C), (D) theta (1000°C), (E) alpha alumina (1200°C).

presence of a high vacuum (assuming the heating effect of the electron beam was negligible) the particles were seen to undergo a morphological change. Electron transmission photographs showed that particle growth took place (up to 13,000 Å diameter) (Figure 7), while diffraction patterns taken of the larger particles showed that they were alpha alumina. This suggests that the gamma phase is less stable at low pressures. The observation of particle growth during the gamma to alpha transformation has been supported by Iler who found that, the alpha crystals once nucleated, grew rapidly to 0.5 to 1.0 μ in size.

To determine if particle growth took place during the formation of the "hard phase" material produced during R.H.P., X-ray line broadening studies were made for

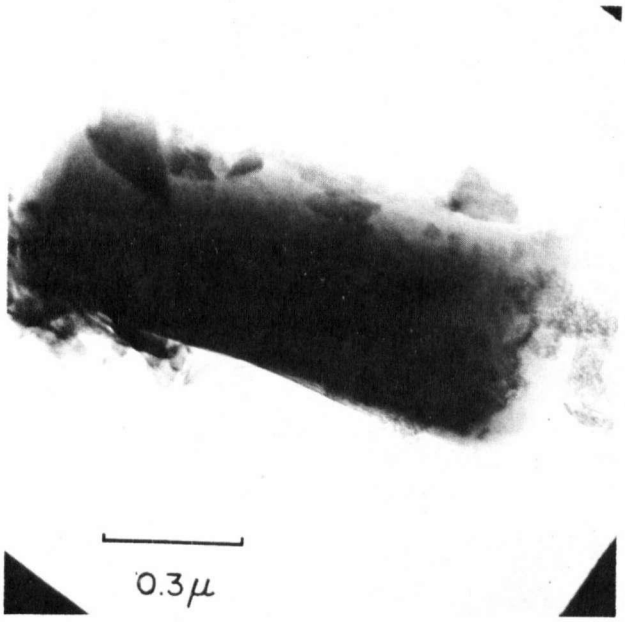

Photo A

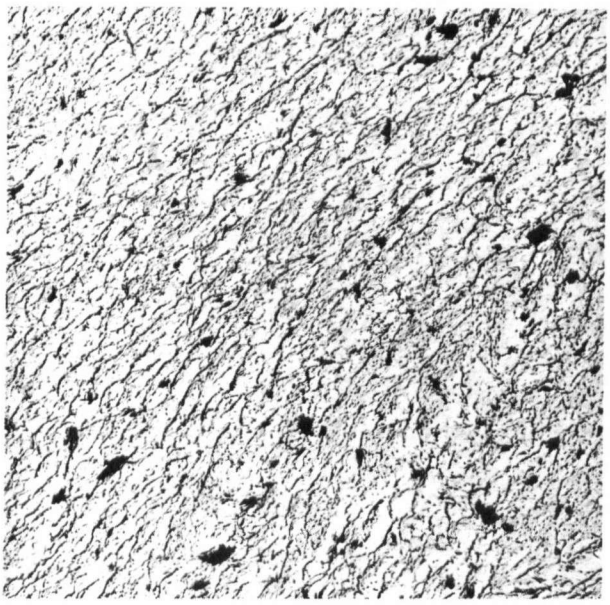

Photo B

Figure 7. Photo A is an electron microscope photo of heat treated boehmite (600°C for 2 hours). X-ray analysis of the material indicated gamma alumina, however, when observed under the electron microscope particle growth had apparently taken place. Electron diffraction analysis indicated the structure of the larger particles to be alpha alumina while the smaller particles gave ring patterns indicating one of the transition aluminas.

Photo B shows a replica of the fracture surface of the hard phase material (x10K).

(i) Bohemite powder which had been heat treated for two hours at 600°C (gamma alumina),

(ii) and compared with the "hard phase" material (gamma alumina, point 14, Figure 4), which was formed during R.H.P.

For the X-ray diffractometer (13) used in these experiments, the focal spot was viewed laterally and the vertical divergence was limited by using Soller slits. Therefore, Figure 8 can be used to correct X-ray diffractometer line breadth for instrumental broadening (12). Figure 8 is valid to the extent that the diffraction line profiles are of the form $1/(1 + K^2\varepsilon^2)$.

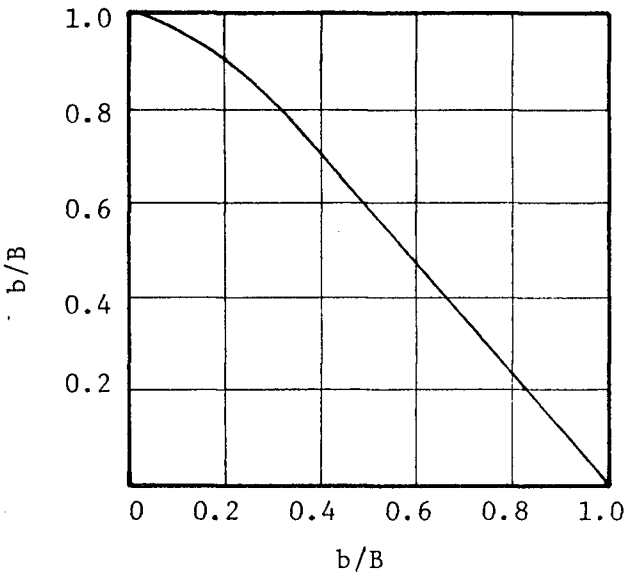

Figure 8. Curve for correcting X-ray spectrometer line breadths for instrumental broadening.

K_α doublet broadening can be corrected for by using Jones' method (Figure 9). In Figure 9 curve "B" was used which can generally be applied to both Debye-Scherrer and X-ray diffraction patterns when "b" and "B" are defined as half maximum breadth. The following nomenclature has been used.

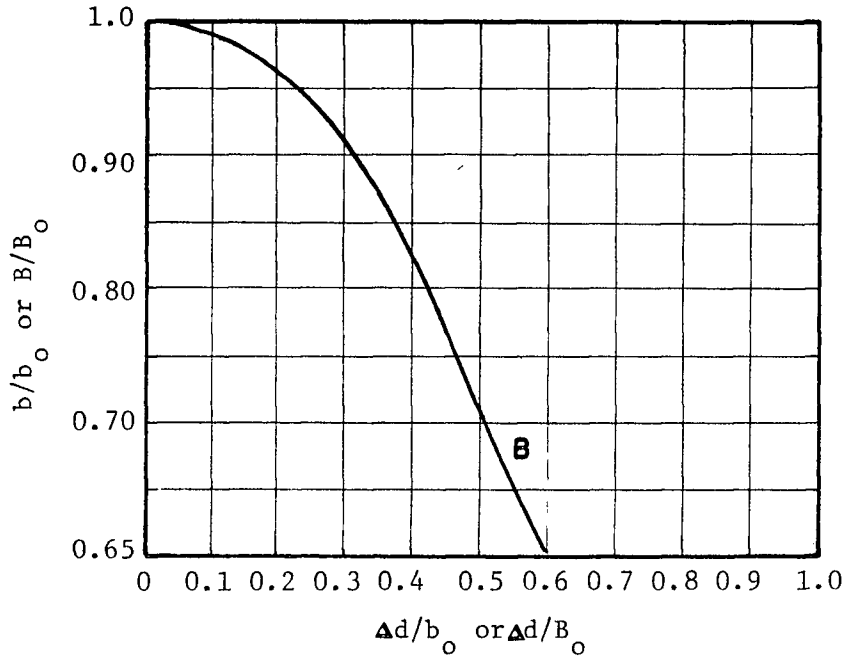

Figure 9. Curve for correcting line breadths for K_α doublet broadening.

"B" = total line breadth due to instrument and crystallite size

"b" = instrumental broadening

"β" = breadth of purer diffraction profile

"B_o" = total line breadth due to instrumental, crystallite size and "K" doublet

"b_o" = total instrumental broadening due to "K" doublet.

To determine the instrument broadening the silicon line at 2θ = 47.34° was used where b_o = 0.28° (see Figures 10a to d). First this line was corrected for "K" doublet broadening. From table (II) $\Delta 2\theta$ = 0.126° = Δd. From Figure 9 using curve B

$$\frac{\Delta d}{b_o} = \frac{0.126}{0.28} = 0.45$$

$$\frac{b}{b_o} = 0.77 \quad \text{giving } b = [0.76][0.28] = 0.21°$$

Comparing Figure 10a, this is approximately the same value one would obtain by extrapolating along the dashed curve (b = 0.18°). Therefore, b = 0.20° has been used as an average. To study the particle size of the heat treated boehmite and hard phase material, the d = 1.997 Å and d = 1.395 Å lines were used. The correction for K_α doublet broadening is shown in Table II.

			heat treated boehmite gamma alumina 600°C for 2 hours			"hard phase" material formed during R.H.P. 700°C		
"d"	"2θ"	Δd= Δ2θ	B_o	$\Delta d/B_o$	B	B_o	Δd/B	B
1.98	45.86	0.12°	2.62	0.725	2.60	1.04°	0.115	1.02°
1.395	67.0	0.19°	-	-	-	1.83°	0.104	1.8°

Table II. Correction for K_α doublet using Figure 9.

The line can now be corrected for instrument broadening using Figure 8. The results are shown in Table III.

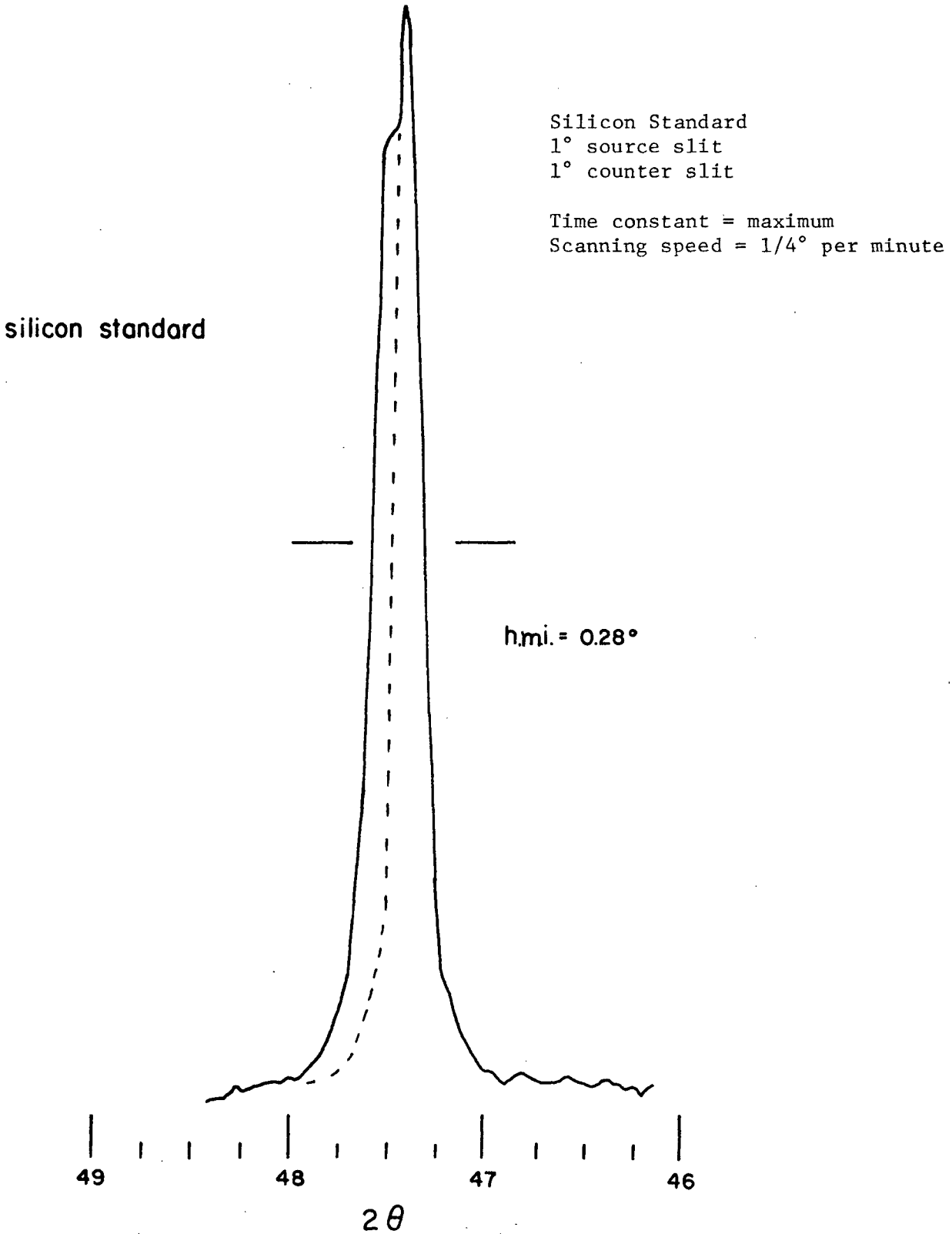

Figure 10a. The silicon line at 2θ = 47.34°, used to obtain instrument line broadening.

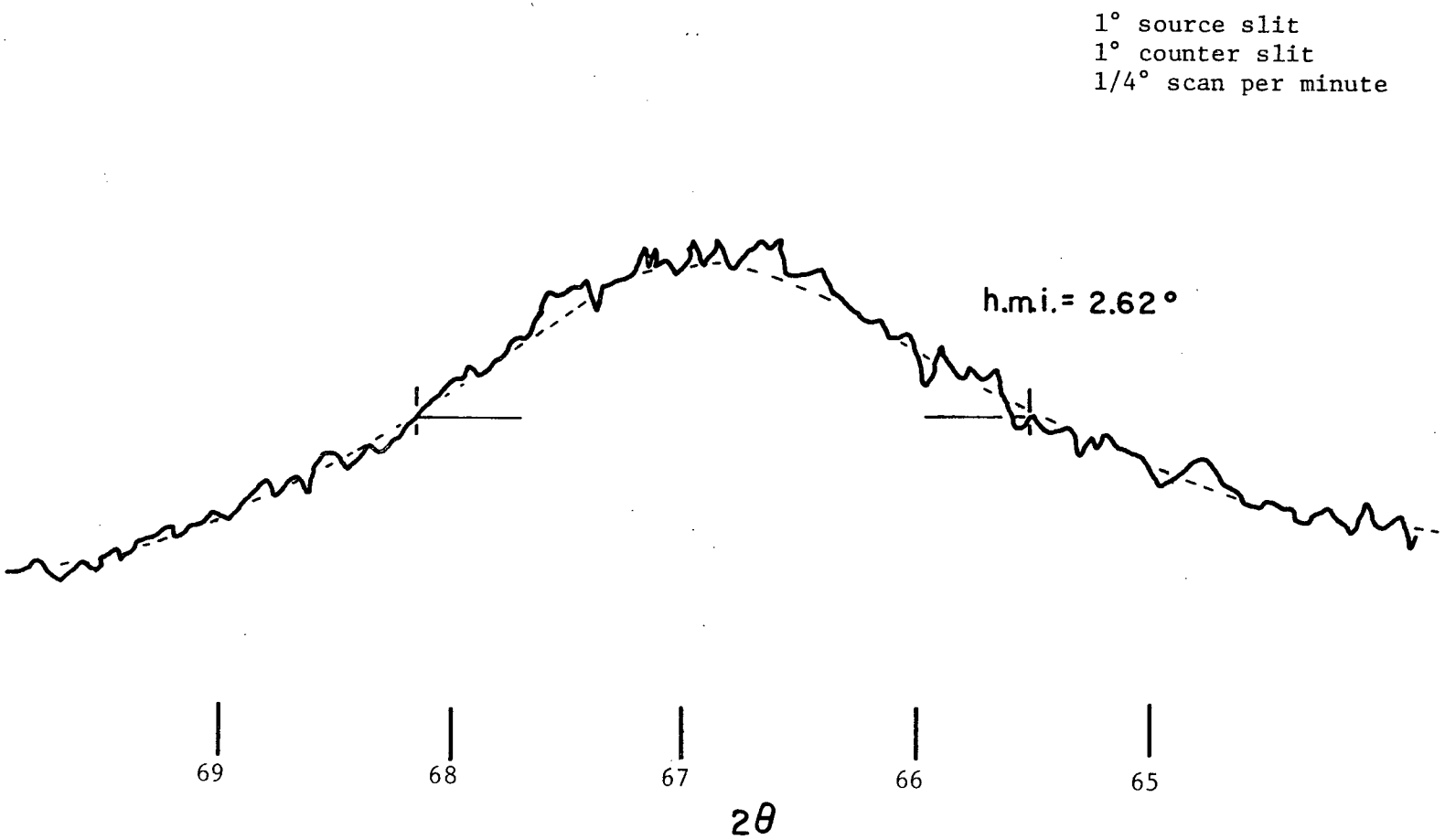

Figure 10b. The diffraction peak at 2θ = 67° for boehmite powder which has been heat treated at 650°C for 2 hours [gamma alumina].

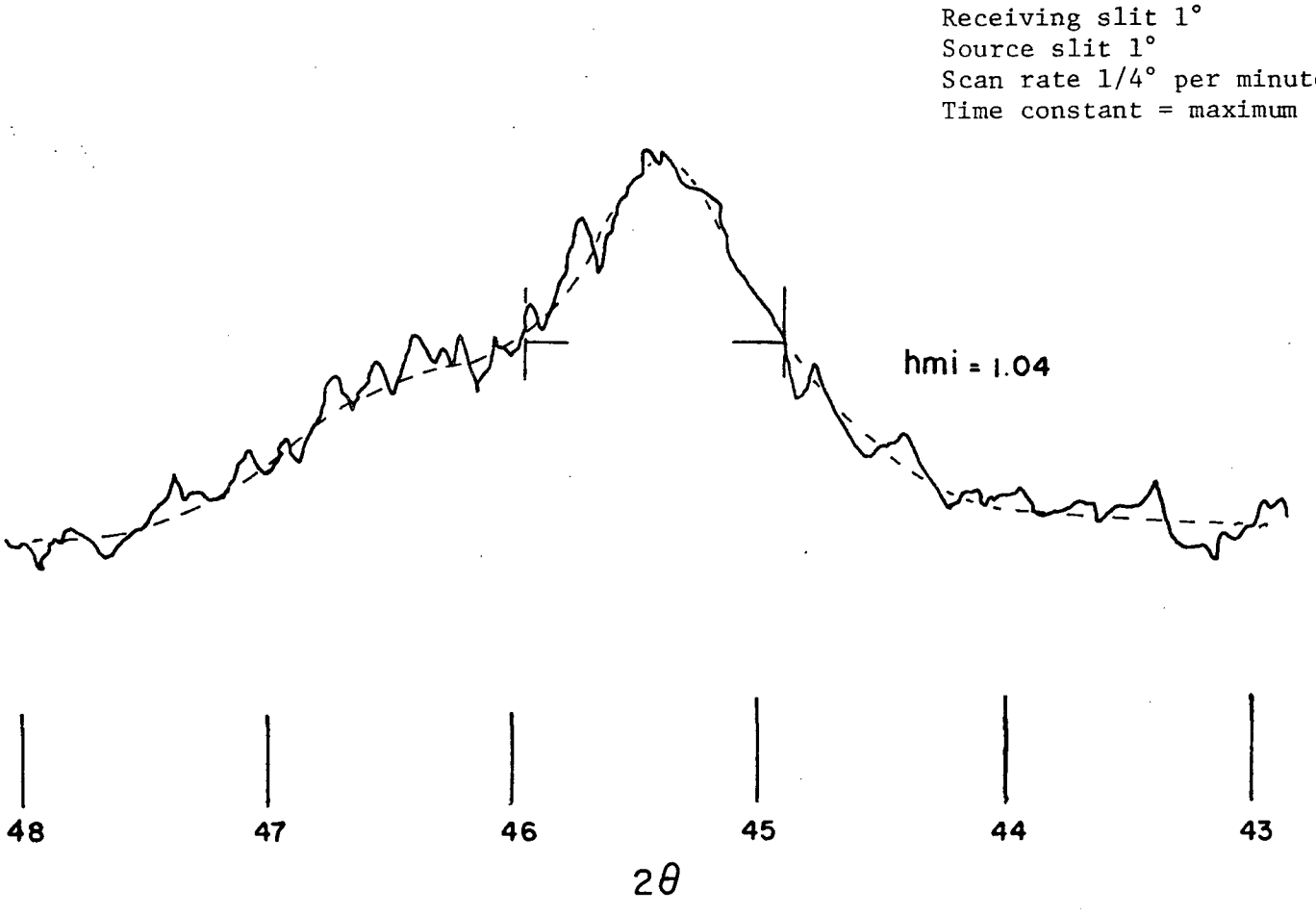

Figure 10c. The diffraction peak at 2θ = 45.3° for the hard crystalline material from specimen 1.

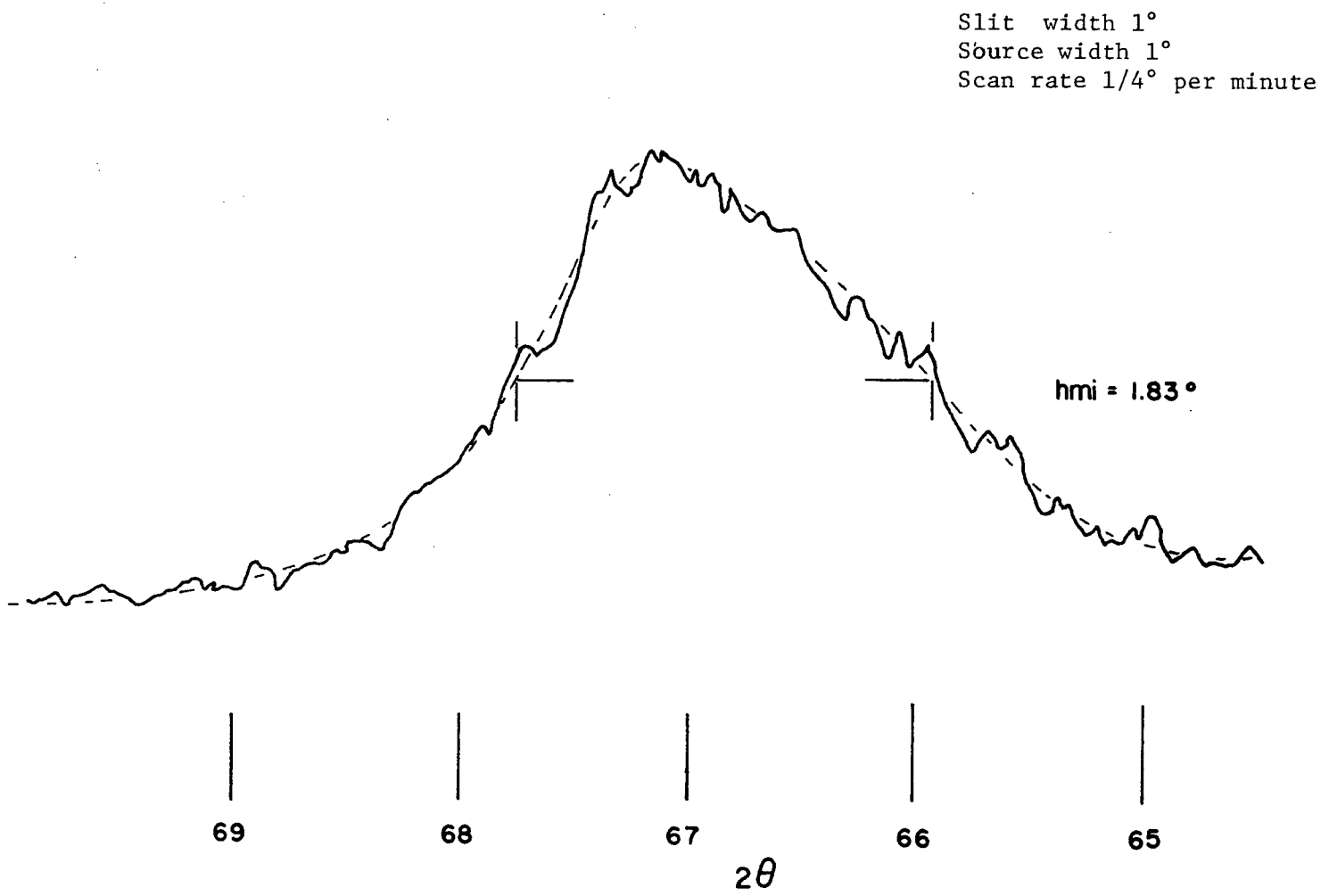

Figure 10d. The diffraction peak at 2θ = 67° for the hard crystalline material from specimen 1.

	heat treated boehmite gamma alumina 600°C for 2 hours				"hard phase" material formed during R.H.P. 700°C			
"d"	B	b/B b=0.20	β/B	β	B	b/B	β/B	β
1.98	2.60	0.77	0.97	2.52	1.02°	0.196	0.90	0.92°
1.395	-	-	-	-	1.8°	0.111	0.98	1.77°

Table III. Correction for instrumental broadening using Figure 8.

The crystallite size was determined using the Scherrer formula

$$D = \frac{K \cdot \lambda}{\beta \cdot \cos(\theta)}$$

The value of "K" ranges from 0.70 to 1.70 depending upon

a. the crystallite shape

b. particular definition of (h.m.i. or integral breadth)

and c. indices of (h, k, 1) reflection planes.

For this work and the nature of the particles being studied, K = 0.9, was used. The results of the line broadening calculations are

For

gamma powder [heat treated boehmite - 600°C for 2 hours]

$$D_{440} = \frac{[0.9][1.542][57.3]}{[2.52]\cos(33.7°)} = 38 \text{ Å} \quad \text{(diameter of fiber)}$$

"hard phase" material

$$D_{400} = \frac{(0.9)(1.542)(57.3)}{(0.92)\cos(22.9°)} = 95 \text{ Å}$$

$$D_{440} = \frac{(0.9)(1.542)(57.3)}{(1.77)\cos(33.7°)} = 53 \text{ Å} \quad \text{(diameter of fiber)}$$

In summary, boehmite powder when heat treated at atmospheric pressure was converted to gamma alumina at approximately 500°C. Once it was converted to the gamma form, it did not transform to alpha alumina until 1200°C. During the boehmite to gamma alumina transformation very little particle growth, if any, took place. Excessive particle growth did not occur until the material was converted to the alpha form. Examination of the small gamma alumina particles under the electron microscope appeared to induce a morphological change (high vacuum environment), transforming the gamma to much larger alpha particles. On the other hand, X-ray line broadening studies of the "hard phase" material produced at the outer edges of specimen 1, showed that no particle growth took place. X-ray studies of both the heat treated boehmite powder and the "hard gamma phase" could not explain why the center of the hot pressed compact had converted to alpha alumina at 700°C. This will be discussed in Section 4.1.

3.4 Thermogravimetric Analysis (T.G.A.)

For this analysis, a Dupont 950 T.G.A. unit was used. The instrument consists of a delicate balance positioned inside a furnace which can be heated at a controlled rate. The device measures the weight loss of an unknown sample as a function of temperature, or under isothermal conditions. The chemical analysis for Baymal boehmite is

AlOOH	83.1 weight %
Acetate	9.8 "
Chemical bond water	3.3 "
Physical adsorbed water	1.8 "
$SO_4^=$	1.7 "

The fractional weight loss (due to dehydroxylation) for the conversion of pure boehmite (AlOOH) to gamma alumina is 0.15 ($Al_2O_3 \cdot H_2O \rightarrow Al_2O_3 + H_2O$). Therefore the total weight loss for boehmite and impurities to gamma alumina should be 29% [9.8 + 3.3 + 1.8 + 1.7 + 12.4 (15% of 83.1)]. The total measured weight loss can be determined from the T.G.A. (Figure 11) and is

Fractional wt. loss [upon heating to 800°C] = 0.304

Assuming that above 200°C all impurities (acetate, b.p. = 118.5°C and $SO_4^=$) have been driven off, one can calculate the fractional weight loss due to water only.

Wt. of sample which is $Al_2O_3 \cdot XH_2O$ = [total wt.]-[wt. of impurities]

= 5.40 - [0.529 + 0.0917] = 4.78 mg

Where

$$\begin{bmatrix} \text{Acetate} = 9.8\% \times 5.4 = 0.529 \text{ mg} \\ SO_4 = 1.7\% \times 5.4 = 0.0918 \text{ mg} \end{bmatrix}$$

therefore

$$\text{Wt. loss (due to water only)} = \frac{4.78-3.76}{4.78} = 0.2113$$

for the reaction $Al_2O_3.XH_2O \rightarrow Al_2O_3 + XH_2O$ gives

$$X = \frac{[102][0.2113]}{[18][1 - 0.2113]} = 1.52$$

suggesting the formula for Baymal boehmite is $Al_2O_3 \cdot 1.5H_2O$.

The fractional weight loss for each region a, b, c, and d can be determined from the T.G.A. curve and the corresponding x's can be calculated using the formula

$$\text{Fractional wt. loss} = \frac{xH_2O}{Al_2O_3 \cdot yH_2O}$$

The results are summarized in Table IV. Table IV shows that the rate of water loss is greatest during the boehmite to gamma alumina transition at 480°C. It should also be pointed out that during stage "d" 4.0% water is lost. This is after boehmite has been transformed to gamma alumina. Houber and de Boer (14) have suggested that the crystalline structure of gamma alumina probably contains about 3.4% water. Additional water may react with the surface, thus the surface composition

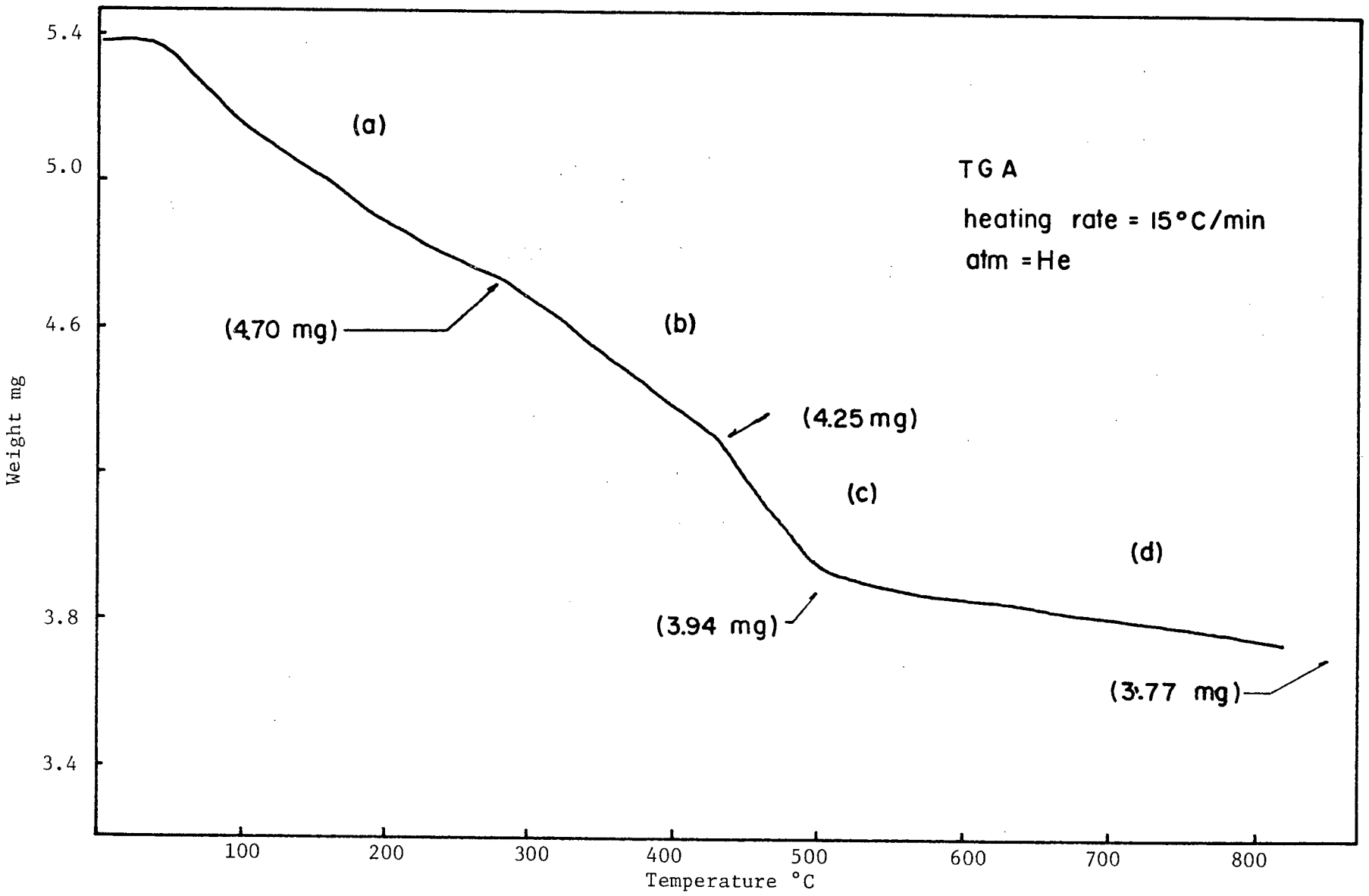

Figure 11. T.G.A. curve for boehmite.

Region	Fractional wt. loss (f)	y	$X = \frac{f[102+18y]}{18}$	Chemical formula	$\frac{d(wt)}{dT°}$ mg/°C
A	$\frac{4.78-4.70}{4.78} = 0.0167$	1.52	0.120	$Al_2O_3 \cdot 1.5H_2O \rightarrow Al_2O_3 \cdot 1.4H_2O + 0.1H_2O$	-
B	$\frac{4.70-4.25}{4.70} = .0957$	1.40	0.676	$Al_2O_3 \cdot 1.4H_2O \rightarrow Al_2O_3 \cdot 0.7\ H_2O + 0.7\ H_2O$	3.08×10^{-3}
C	$\frac{4.25-3.04}{4.25} = .0729$	0.724	0.4659	$Al_2O_3 \cdot 0.7\ H_2O \rightarrow Al_2O_3 \cdot 0.8\ H_2O + 0.4\ H_2O$	6.84×10^{-3}
D	$\frac{3.94-3.77}{3.94} = .0431$	0.258	0.2554	$Al_2O_3 \cdot 0.3\ H_2O \rightarrow Al_2O_3 + 0.3H_2O$	0.625×10^{-3}

Table IV. Analysis of T.G.A. data.

$$Al_2O_3.yH_2O \rightarrow Al_2O_3.(y-x)H_2O + xH_2O$$

is given by AlOOH while the internal structure is HAl_5O_8. While others have suggested that any water associated with gamma alumina must exist on the surface only.

3.5 D.T.A.

D.T.A. stands for differential thermal analysis. Differential thermal analysis was used for studying the physical and chemical changes of boehmite during heating. The principle of the device is simple. Thermocouple "A" is placed in a sample of material to be analyzed.

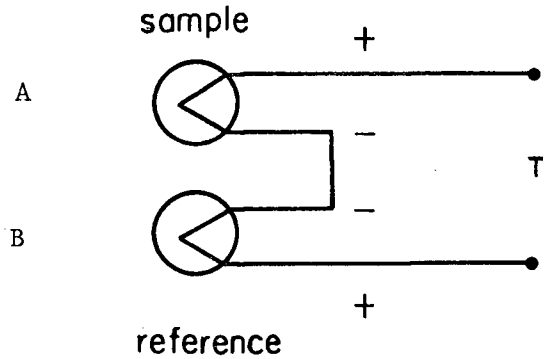

Thermocouple "B" is placed in an inert reference material, which has been selected so that it will not undergo any thermal transformation over the temperature range being studied. When the temperature of the sample equals the temperature of the reference material, the two thermal couples produce identical voltages (emf), the net voltage output is zero. However, when the sample goes through a transformation where heat is evolved or absorbed, the thermocouple "A" either reads higher or lower than thermocouple "B", this results in a net voltage

differential which is recorded as a temperature differential.

3.5.1 Discussion of Figure 12

Figure 12 is a D.T.A. curve for Baymal boehmite. The first endothermic peak at approximately 108°C is due to decomposition of impurities such as acetate (acetic acid, b.p. = 118°C). The peak at 275°C is a baseline peak corresponding to a change in the rate of dehydroxylation of boehmite and not an exothermic peak as one might conclude at a first glance. Therefore the region from 275°C to 381°C must be endothermic. This is more realistic since in this region water is being lost, which is an endothermic reaction (see Figure 12). Regions I and II are characterized by the same rate of weight loss, however, from 381°C to 443°C there is an exothermic baseline shift. A shift of baseline in the exothermic direction may be due to an increase in thermal conductivity, a decrease in heat capacity of the sample, or it may result from the sintering of particles (15). From 443°C to 481°C, the transformation region, there exists a large endothermic peak. This is due to the phase transformation of boehmite to gamma alumina with the attendant loss of water.

3.6 Isothermal Compaction Curves for Boehmite

Figure 13 shows a series of isothermal compaction curves ($\frac{\Delta L}{L_o}$ versus time), which were obtained by applying a constant pressure (σ_{ref}) at a given temperature. Each curve can be expressed as a sum of exponentials of the form

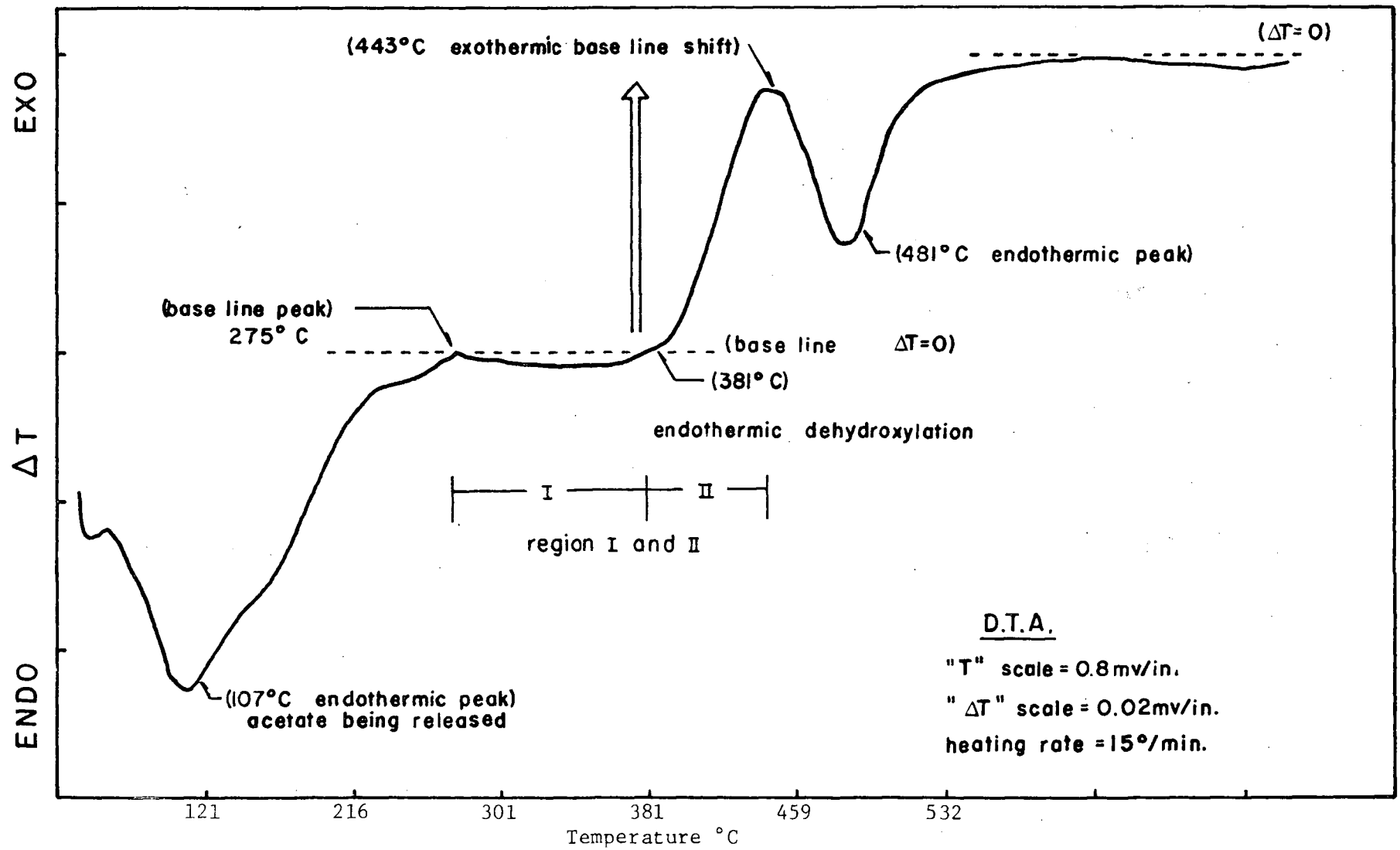

Figure 12. D.T.A. for boehmite (plat. versus plat. +13% rhodium thermocouple).

$$\frac{\Delta L}{L_o} = K(1 - Ae^{-\alpha t} - Be^{-\beta t}) \qquad (1)$$

where K, A, α, B and β are constants which can be uniquely determined (see Table VII).

"$\frac{\Delta L}{L_o}$" is the strain (compaction) = ε

"t" the time

$K = \{\frac{\Delta L}{L_o}\}_{t=\infty}$ or the final compaction

A and B are constants for which the following condition must be satisfied

at time = 0, $(\frac{\Delta L}{L_o})_{t=0} = 0$ i.e., A + B = 1

3.7 The Experimental Determination of the Constants K, α, A, B, and β

The constant "α" can be uniquely determined by assuming that $\beta >> \alpha$. Thus for time much greater than zero, the contribution from one of the exponential terms will be approximately equal to zero. Taking the derivative of equation (1) one obtains

$$\frac{d\varepsilon}{dt} = K\{A\alpha e^{-\alpha t} + \beta B e^{-\beta t}\} \qquad (2)$$

if $\beta >> \alpha$ then for $t >> 0$

$$\frac{d\varepsilon}{dt} \simeq KA\alpha e^{-\alpha t}$$

or $$\ln\left(\frac{d\varepsilon}{dt}\right) = -\alpha t + \ln\{KA\alpha\} \qquad (3)$$

Figure 14a shows "$\frac{\Delta L}{L_o}$" versus "t" for run 27, an isothermal compaction curve for boehmite at 498°C. From this graph the natural logarithm of the slope versus time was plotted (see Figure 14b). Data was only used for time > 3 minutes. From the slope of Figure 14b the value of "α" can be determined, and from the intercept "A" can be calculated since, intercept = $\ln\{K\alpha A\}$. The constant "B" can then be determined using $A + B = 1$. To determine "β", the constants K, α, A, B and the corresponding experimental $\frac{\Delta L}{L_o}$ are substituted into equation (1) for time equal to one minute. Hence, the compaction of boehmite at 498°C can be expressed mathematically as

$$\frac{\Delta L}{L_o} = (0.112)(1-0.472e^{-0.19t} - 0.528e^{-2.87t}) \qquad (4)$$

The same procedure was repeated for Figures 15a to 15h. The assumption $\beta >> \alpha$ is justified, since in Figure 14a the natural log of the slope fits a straight line for t > 3 minutes.

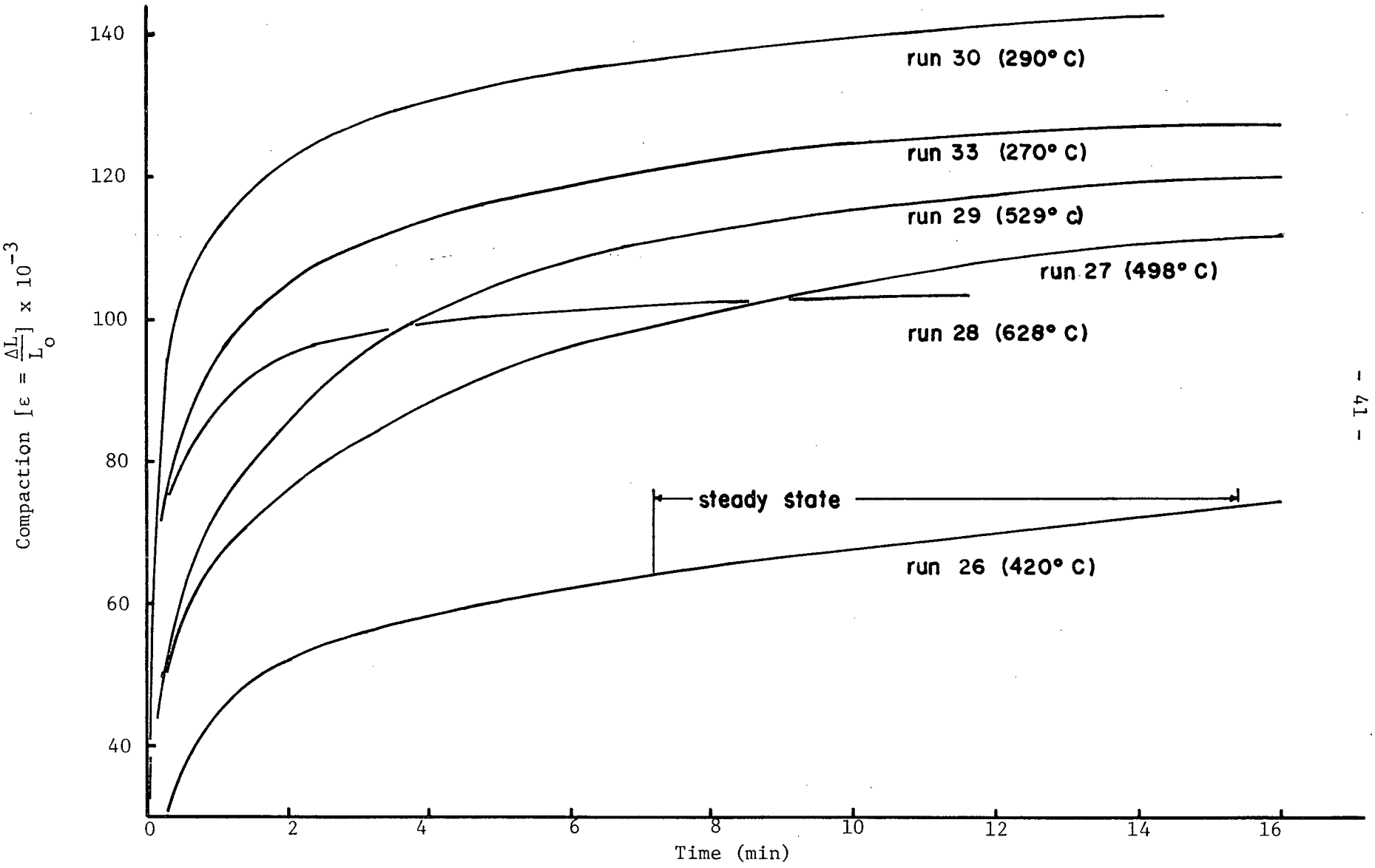

Figure 13. Isothermal compaction curves for boehmite (R.H.P. at 5860 psi).

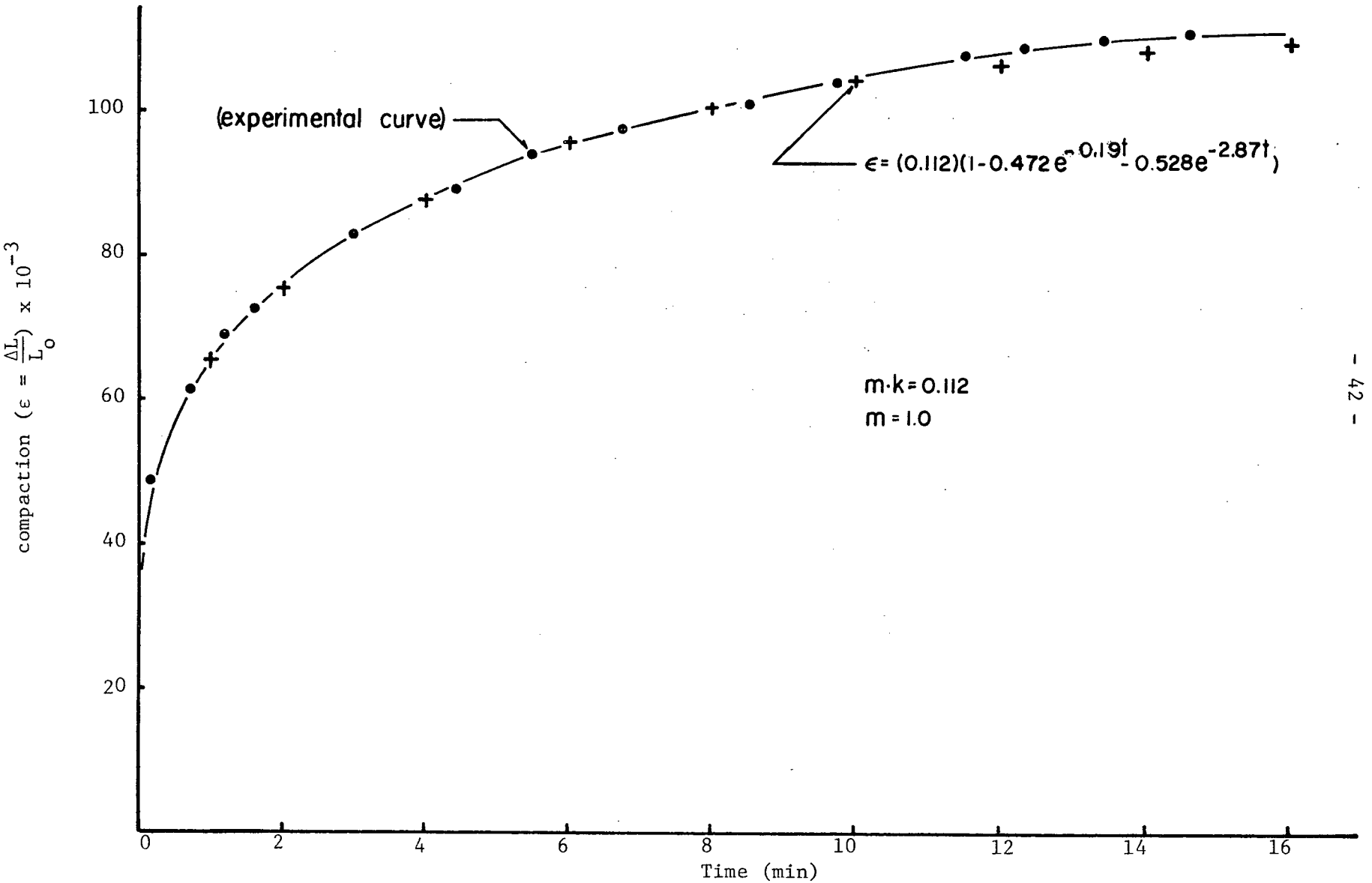

Figure 14a. Run 27 (R.H.P. compaction curve for boehmite at 498°C and 5860 psi).

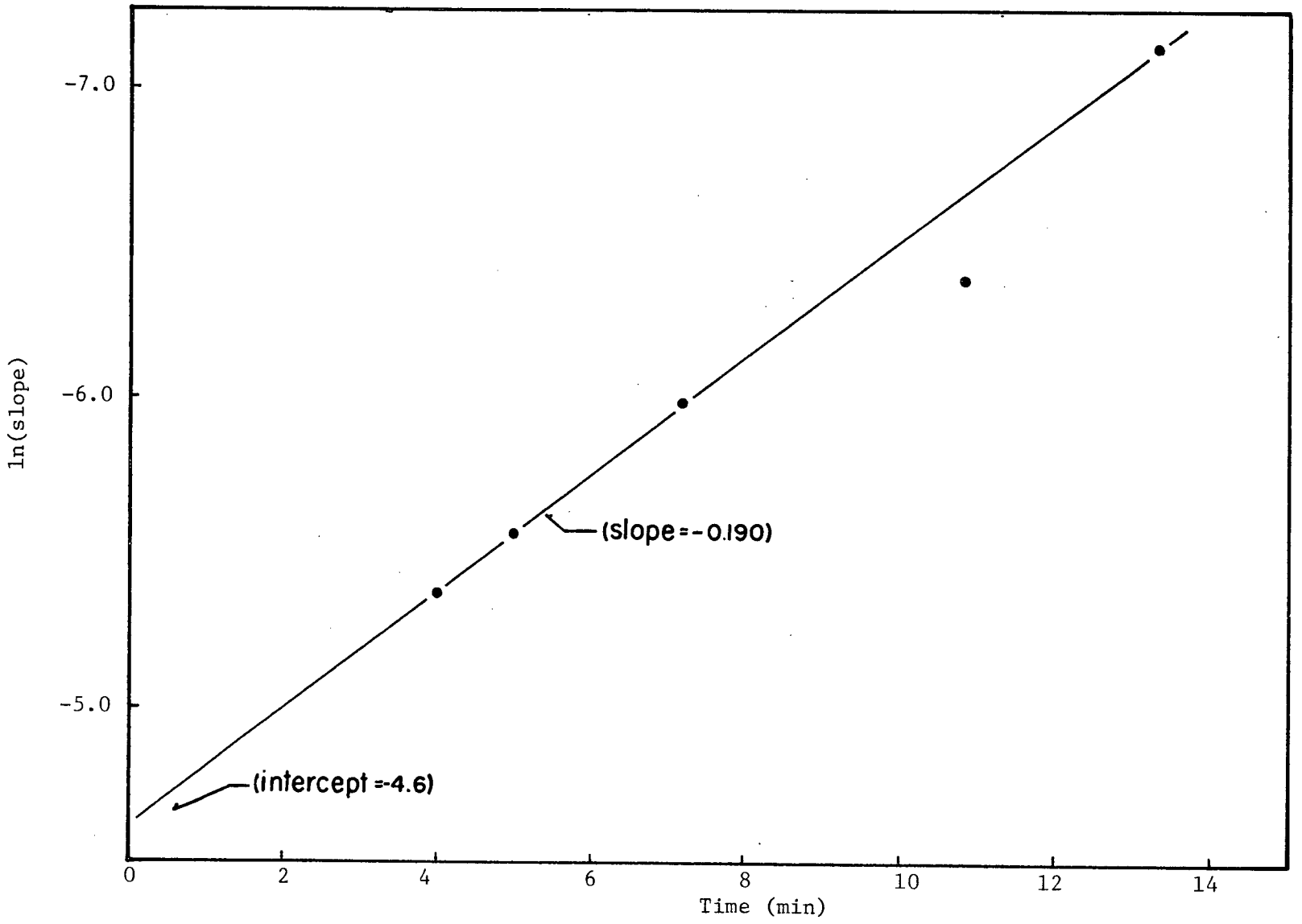

Figure 14b. ln(slope) versus time for run 27 at 498°C.

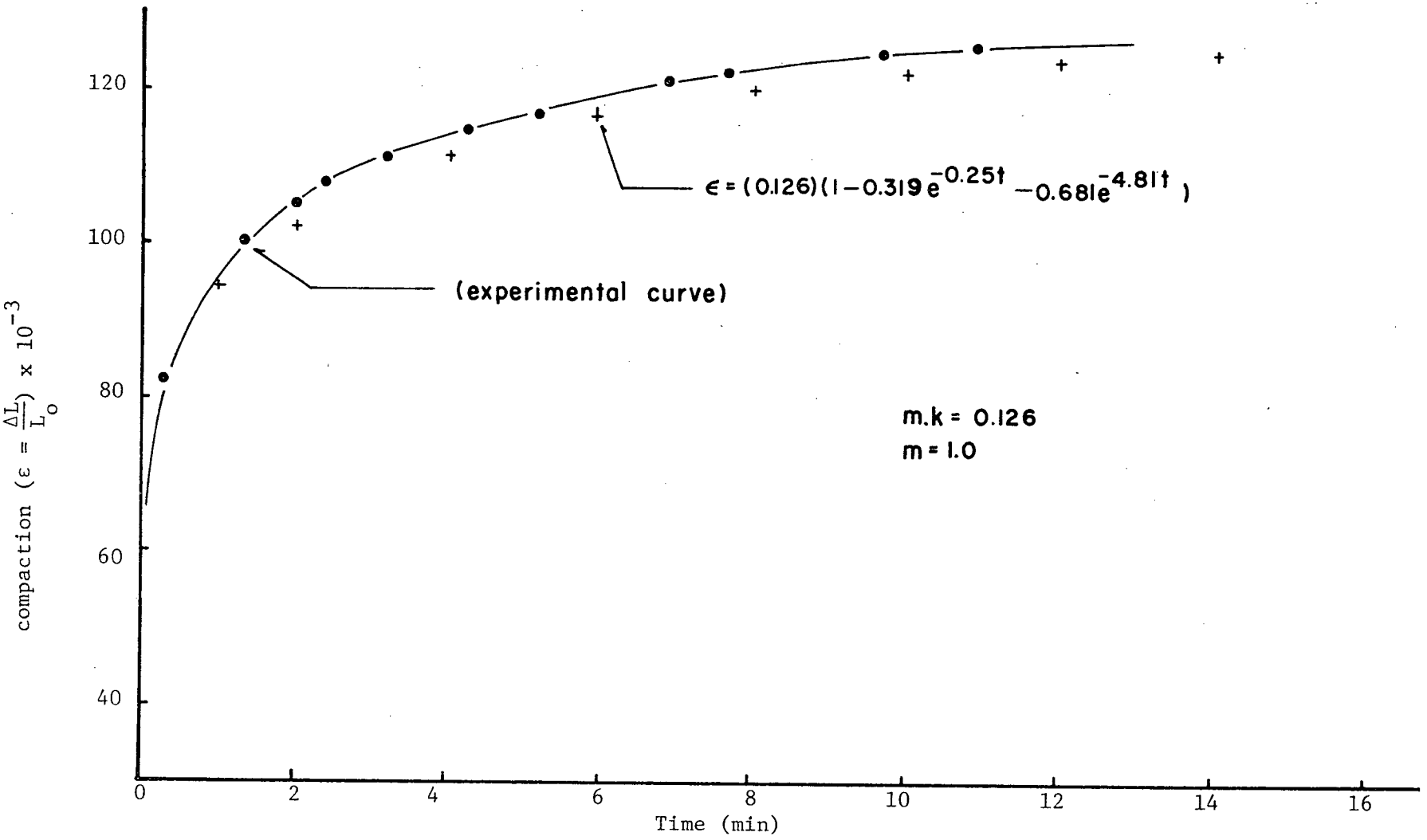

Figure 15a. Run 33 (compaction curve for boehmite at 270°C and 5860 psi).

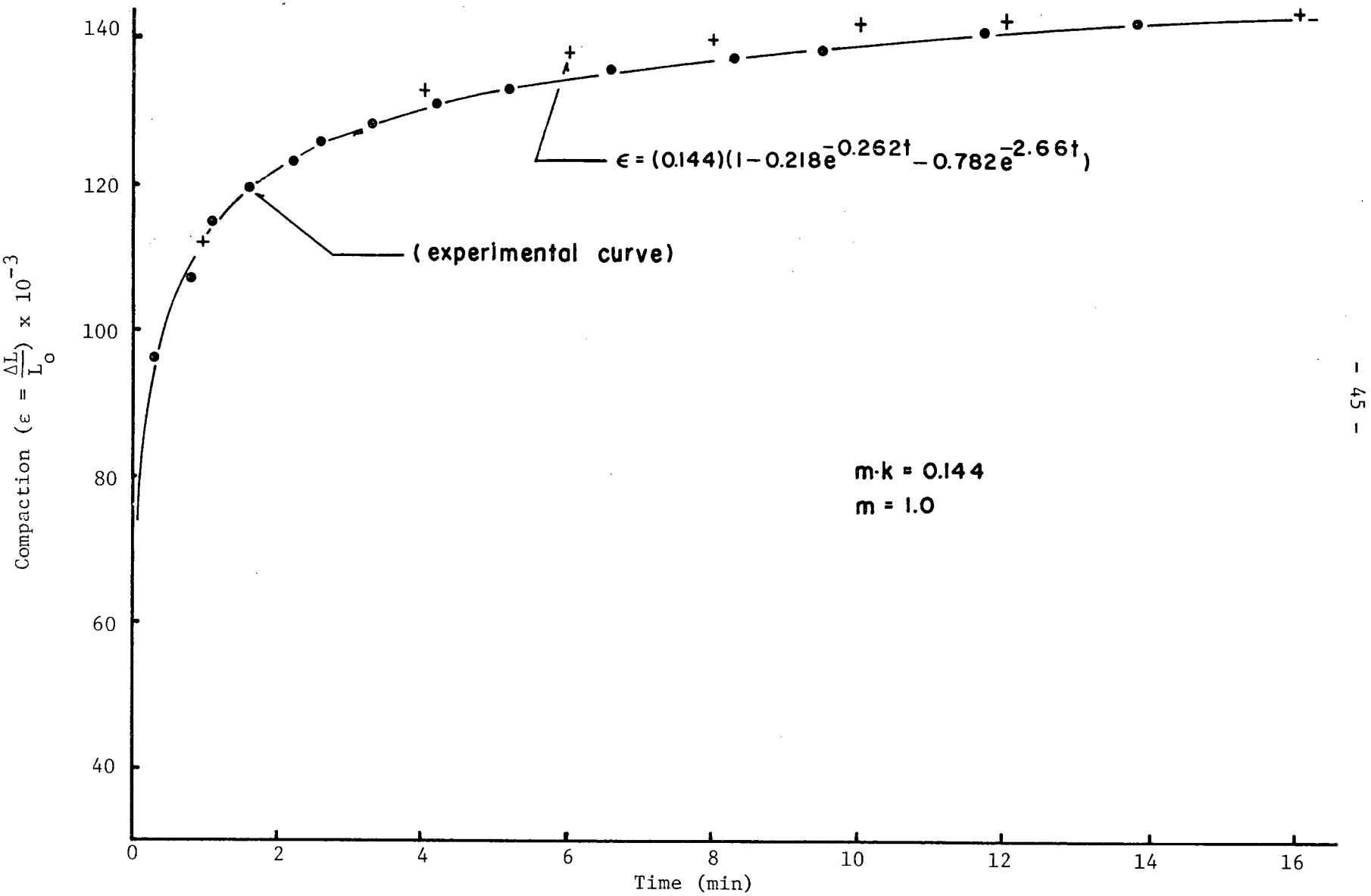

Figure 15b. Run 30 (compaction curve for boehmite at 290°C and 5860 psi).

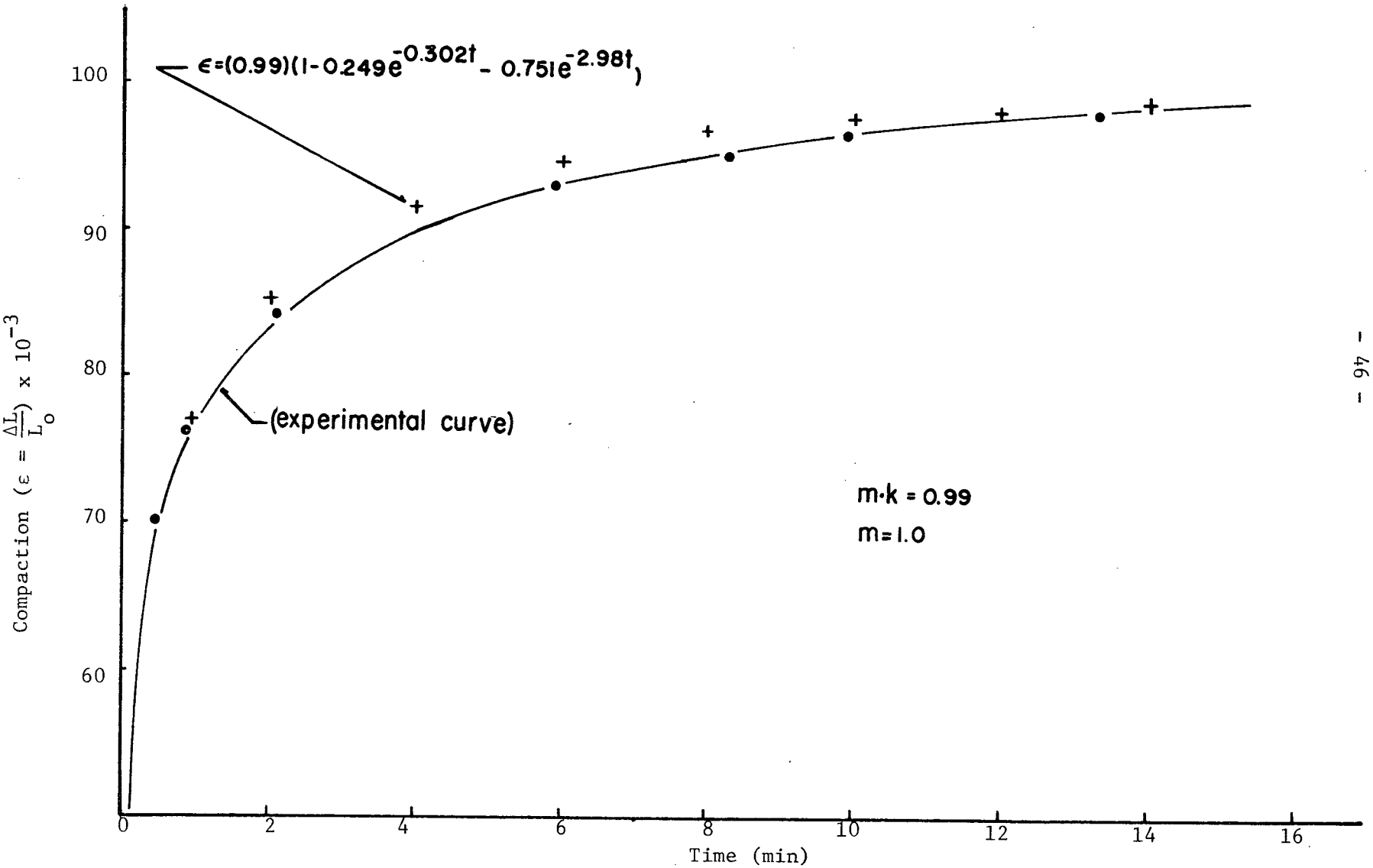

Figure 15c. Run 22 (compaction curve for boehmite at 400°C and 5860 psi).

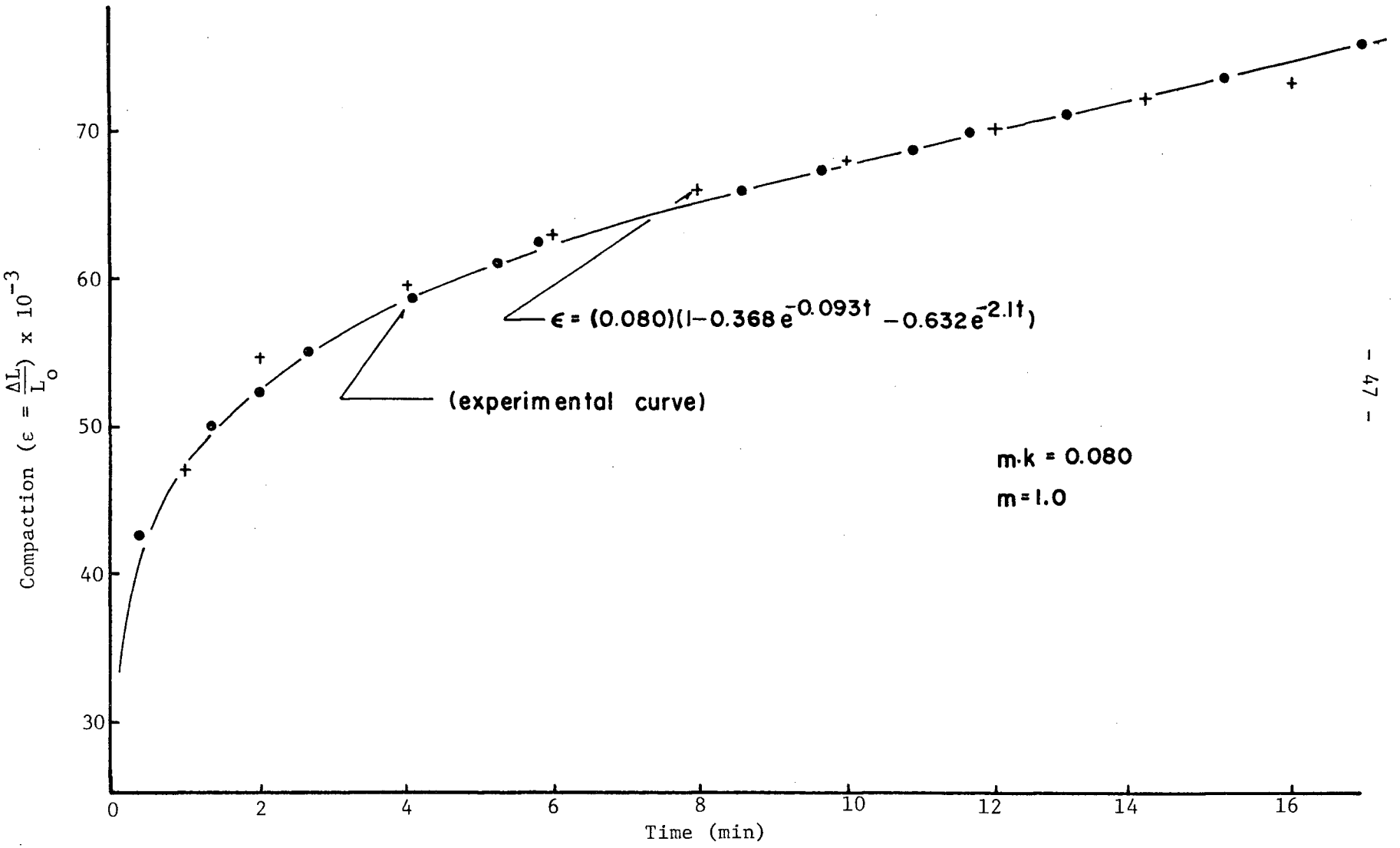

Figure 15d. Run 26 (compaction curve for boehmite at 420°C and 5860 psi).

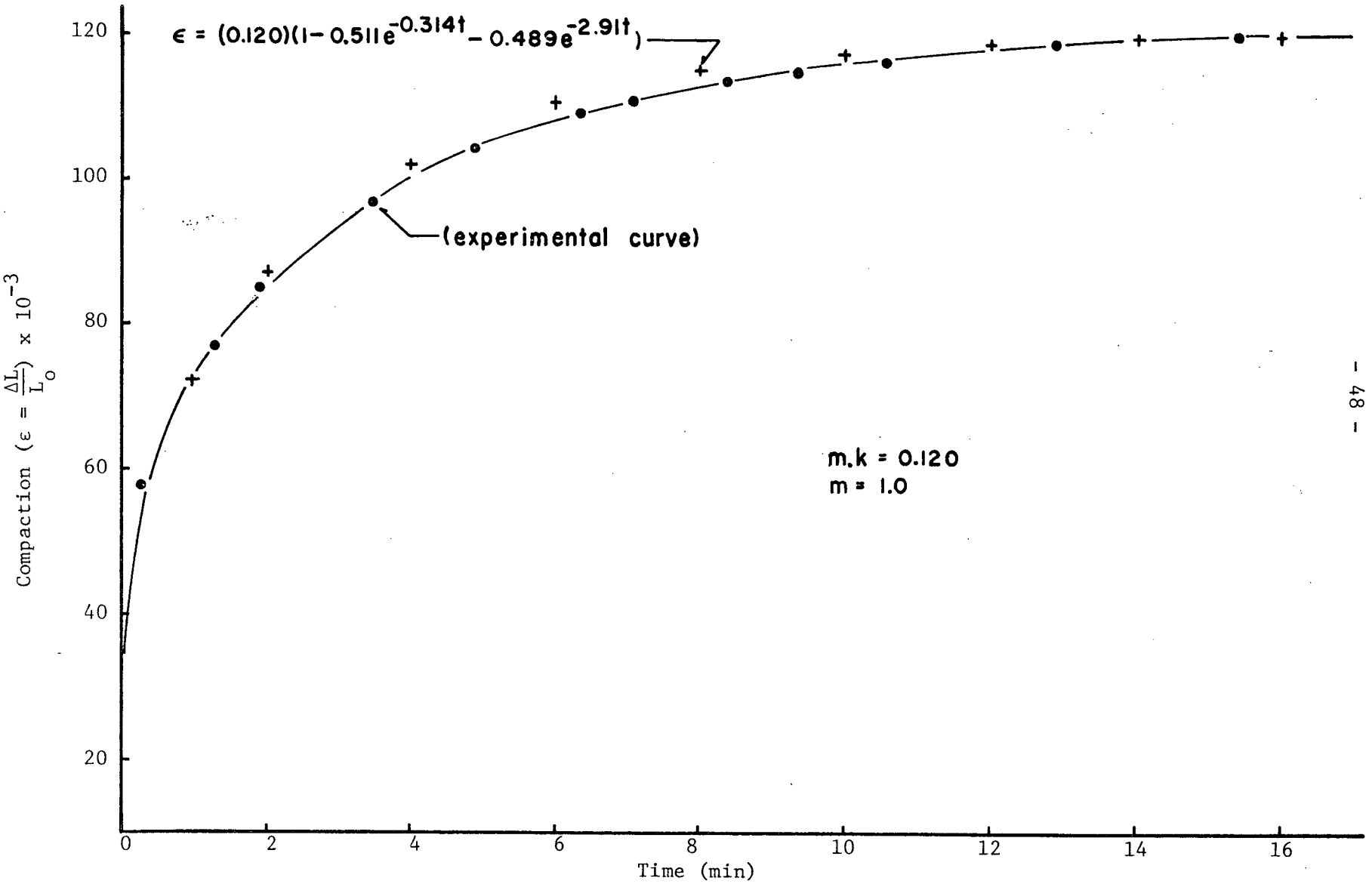

Figure 15e. Run 29 (compaction curve for boehmite at 529°C and 5860 psi).

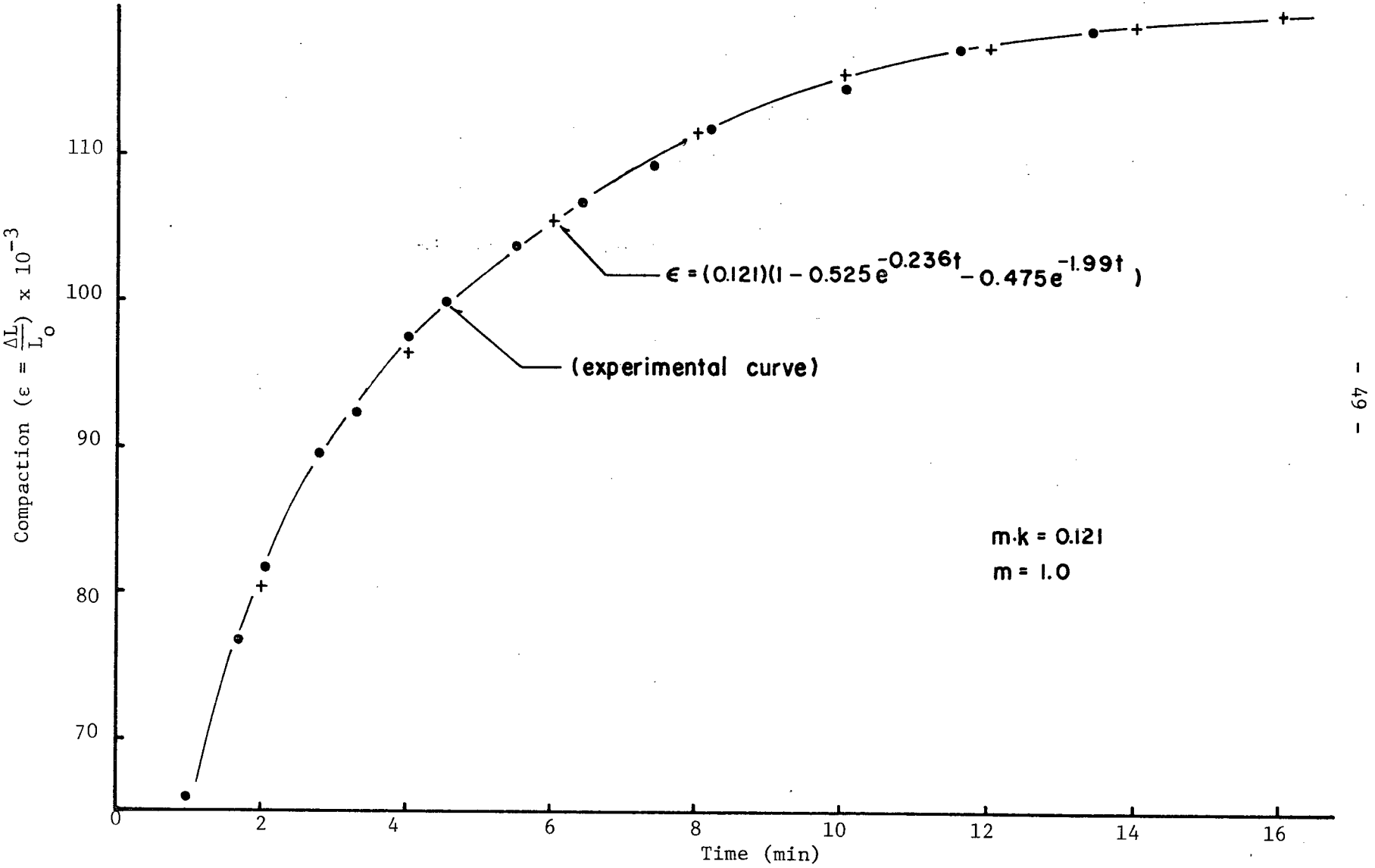

Figure 15f. Run 15 (compaction curve for boehmite at 540°C and 5860 psi).

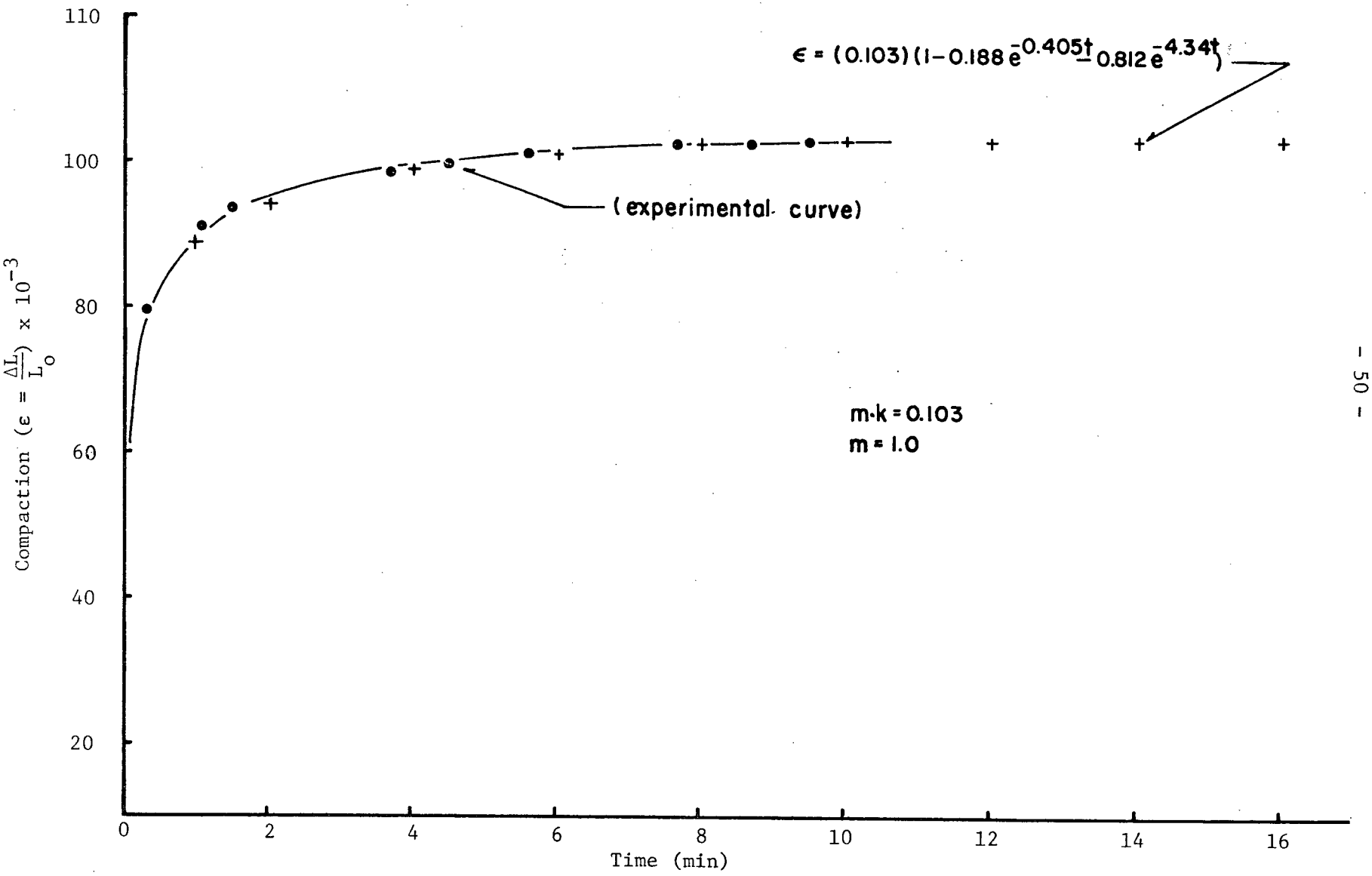

Figure 15g. Run 28 (compaction curve for boehmite at 628°C and 5860 psi).

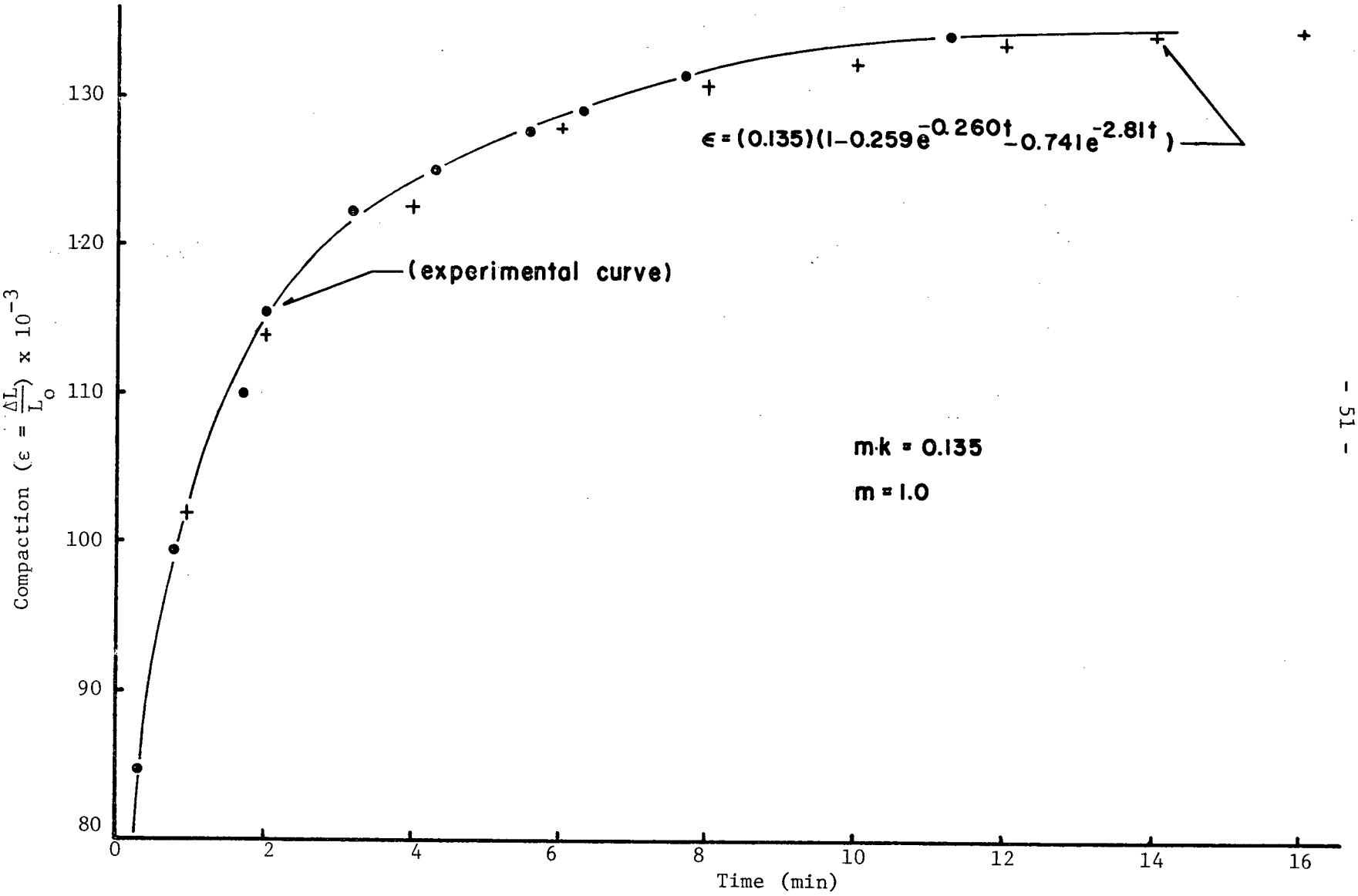

Figure 15h. Run 23 (compaction curve for boehmite at 622°C and 5860 psi).

4. DISCUSSION

4.1 Formation of the Hard Phase Material

When boehmite was R.H.P. at 700°C and under 8000 psi, it was found that a "hard phase" material could be produced. X-ray analyses indicated that its structure was gamma alumina and that no apparent grain growth had taken place during its formation. For the same compact, (Figure 4) the central region had been converted to alpha alumina and apparently there was excessive particle growth. Contrary to what was expected, alpha alumina - the high temperature phase, was formed in the cooler or central regions of the compact.

The phenomenon can be explained if the effect of water vapor pressure is taken into account. Since the vapor pressure would be greatest at the center of the compact, pressure could either reduce the gamma to alpha transition temperature according to Clapeyron's equation. Or secondly, the vapor pressure causes the boehmite to transform directly to alpha alumina without the formation of the intermediate gamma phase. The latter explanation is preferred on the basis of a calculation which showed that to lower the gamma to alpha transition to 500°C, more than a million psi pressure is needed in the system.

Wheat and Carruthers (16) observed the same phenomenon when pressing

$B\text{-}Al_2O_3$ at 20,000 psi and 750°C. They found that the edge of their compacts were composed entirely of gamma alumina, whereas the center consisted of the alpha form only. Also, if one refers to Figure 4, point 16 is a direct evidence of the effect of pressure on the formation of the alpha phase. The fracture crack running from the edge to the center of the compact would act as a pressure sink, allowing the formation of the hard phase closer to the center of the specimen. Also, it becomes obvious that the hard gamma phase was first nucleated at the outer edges where the temperature was highest. As the "hard phase" material started to grow towards the center of the compact, it formed an impermeable barrier preventing the escape of water vapor from the interior of the compact. Due to the increase in water vapor pressure, boehmite in the central region might have converted directly to alpha alumina.

To verify that gamma alumina formed from boehmite at a lower pressure will not convert to alpha alumina below 700°C during R.H.P., boehmite powder was heat treated to 600°C (at atmospheric pressure) to convert it to the gamma form. Then water was added and the material was left to age for 2 hours. After which the material was vacuum dried then R.H.P. at 700°C under 8000 psi. The final compact consisted entirely of gamma alumina, as was expected. The behaviour of boehmite during R.H.P. is schematically represented in Figure 16.

One of the essential findings of this investigation is that, it is the boehmite to gamma alumina transformation that is important in producing "hard phase" material. However, it should be mentioned that when boehmite powder is heat treated (at one atmosphere) to produce gamma alumina,

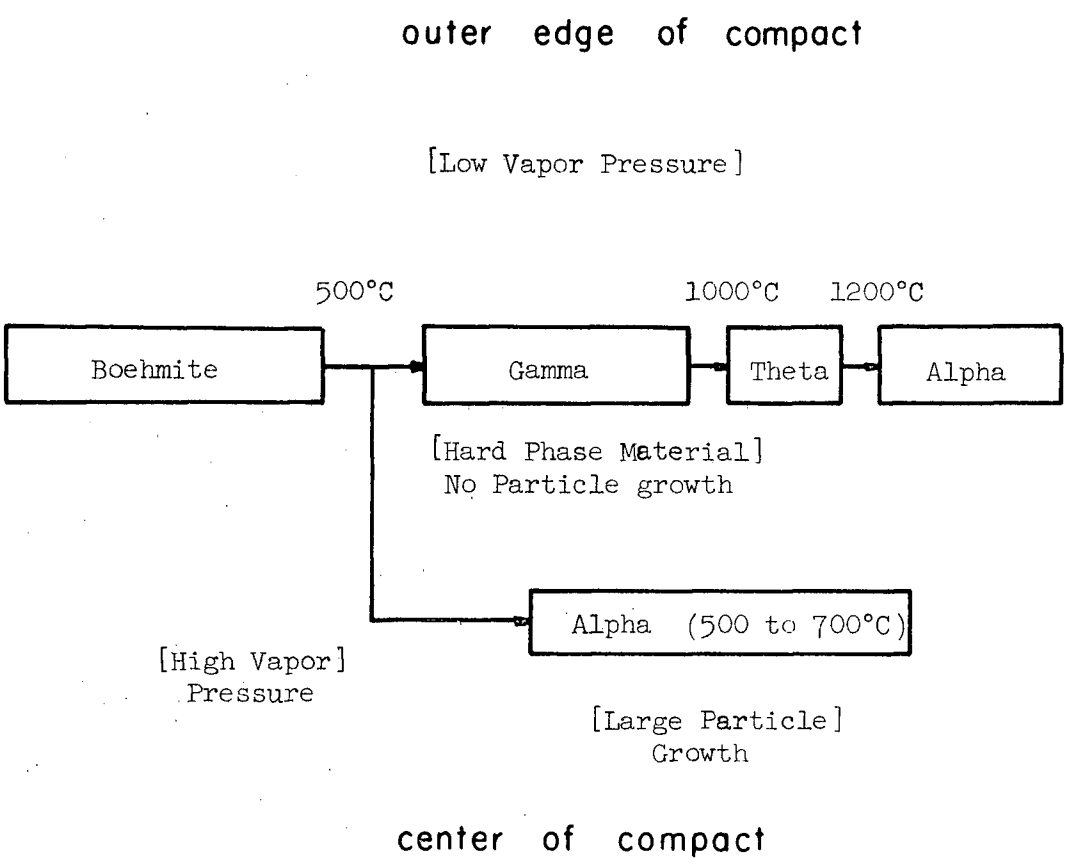

Figure 16. Behaviour of boehmite during R.H.P.

its powder characteristics are exactly the same as the initial starting material. That is, the gamma material is still a finely divided white powder. But when the "hard gamma phase" was formed during R.H.P. it always had a blackish appearance, suggesting that carbon might somehow be involved in the reaction. Carbon was always present during R.H.P., especially when a graphite sleeve was used. However, for the "canning" operation carbon was only present as the impurity acetate. Alternatively, it is also possible that the black appearance

of the "hard phase" is due to an optical phenomenon and not carbon. Other experimenters have observed the same phenomenon in different systems. Their explanation is that the "hard phase" material is translucent, but due to the presence of porosity nests, light is scattered in such a way that the material appears black.

Although, the crystallography of boehmite to gamma alumina change has been worked out in detail, very little is known about the physical and morphological changesassociated with this transformation, except that particle growth does not occur. To obtain a better understanding of the behaviour of boehmite during R.H.P.,isothermal compaction curves were obtained by R.H.P. boehmite in a steel die with sufficient clearance to allow all water vapor to escape. While under these conditions,it was not possible to produce the hard phase material, it did yield more information relevant to the behaviour of boehmite just before and during the gamma transition. These results are discussed in part II in terms of a viscoelastic model.

4.2 The Dynamic System - Part II

As stated before in Section 4.1, data obtained from isothermal compaction curves would be used as an aid in understanding the behaviour of boehmite before and during the gamma transformation. While the compaction data as shown in Figure 13, appears to be somewhat complex in nature, an attempt has been made to relate the data to a simple viscoelastic system as follows.

If a mathematical model is to suitably describe reactive hot pressing, it must be dynamic, that is time varying to any given input (stress, strain, voltage etc.). The simplest dynamic system which

could possibly be related to R.H.P. of boehmite is a second order system (refer to Section 3.6). The output (strain, stress, voltage etc.) can be effectively described by a second order linear differential equation.

The response of a second order system to a unit step input can be described by an equation of the form (19)

$$\varepsilon = K\{1-Ae^{-\alpha t} - Be^{-\beta t}\} \qquad (5)$$

It has been shown in Section 3.6 that the R.H.P. of boehmite can be expressed by a second order system which has the exact form of equation (5) where

"ε" would be the strain $\Delta L/L_o$

"t" the time

$K = (\frac{\Delta L}{L_o})_{t=\infty}$ or $(\frac{\Delta L}{L_o})$ at time equal to infinity

α and β are constants

A and B are constants such that the following conditions must be satisfied.

At time = o, $(\frac{\Delta L}{L_o})_{t=0} = 0$

or $0 = K[1 - A - B]$

giving $A + B = 1$

As the data was obtained as a function of time by heating the powder to a given temperature and applying a constant stress (or pressure), it

can be said that the system is responding as described by equation (5) to an input which can be considered a unit step input. This is explained schematically in Figure 17,

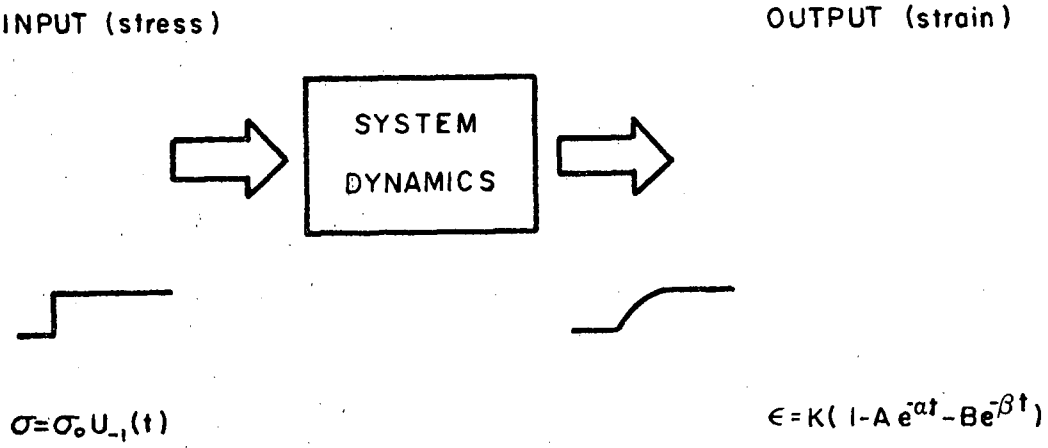

Figure 17. Schematic representation of "system dynamics" relating output (strain) to input (stress).

and mathematically by

$$\varepsilon = x\sigma \tag{6}$$

where ε = strain (output)

σ = stress (input)

x = transfer function

The applied step input was normalized to a given reference stress* or

---

* Note that when $\sigma_{ref} = \sigma_{applied}$ the input is just a unit step function $U_{-1}(t)$. The reference stress chosen for this work was σ_{ref} = 5860 psi.

$$\sigma = \frac{\sigma_{applied}}{\sigma_{ref}} \quad U_{-1}(t)$$

where $U_{-1}(t) = \begin{cases} 0 \text{ for } t < 0 \\ 1 \text{ for } t > 0^+ \end{cases}$

Since the response of the system is known for a given input, the transfer function for the system can now be determined simply by using Laplace transforms.

The procedure is as follows:

(a) From Feedback theory (17), it is known that if the system is linear, then the response of a system to a unit pulse input $U_0(t)$ is just the derivative of the system response for a unit step input $U_{-1}(t)$. For our system since

$$\varepsilon = K\{1-Ae^{-\alpha t} - Be^{-\beta t}\}$$

is the response for a unit step input, then the derivative is the response for a unit impulse, or

$$\frac{d\varepsilon}{dt} = AK\alpha e^{-\alpha t} + K\beta Be^{-\beta t} \tag{8}$$

(b) Using equation (6) and taking the Laplace transform

$$E = X\square^{\dagger} \tag{9}$$

---

† Note capital letters will be used for the Laplace transform. The Laplace transform of any time function is written as $\pounds[f(t)]$ and defined by $\pounds[f(t)] = \int_{t=0^+}^{t=\infty} f(t)e^{-st}\,dt$

where

$$E = \mathcal{L}[\frac{d\epsilon}{dt}] = \frac{a}{S+\alpha} + \frac{b}{S+\beta} = \frac{(a+b)S+a\beta+b\alpha}{S^2+(\alpha+\beta)S+\alpha\beta}$$

and $a = KA\alpha$

$b = KB\beta$

$a\beta+b\alpha = K\alpha\beta$ (boundary condition A + B = 1)

but

$$\square = \mathcal{L}[U_0(t)] = 1$$

Therefore on substitution one obtains the transfer function

$$X = \frac{K[A\alpha+B\beta]S+K\alpha\beta}{S^2+(\alpha+\beta)S+\alpha\beta} = \frac{RS+D}{S^2+HS+T} \qquad (10)$$

In other words,the transfer function which describes R.H.P. of boehmite must have the form of equation (10) where

$$R = K[A\alpha+B\beta] \qquad (11a)$$

$$D = K\alpha\beta \qquad (11b)$$

$$H = \alpha+\beta \qquad (11c)$$

$$T = \alpha\beta \qquad (11d)$$

The second order linear differential equation which has a transfer function of the form (10) can easily be determined by rewriting equation (10) as

$$[S^2+HS+T]E = [RS+D]\square \qquad (12)$$

and then taking the inverse Laplace transform, one obtains

$$\frac{d^2\varepsilon}{dt^2} + H\frac{d\varepsilon}{dt} + T\varepsilon = R\frac{d\sigma}{dt} + D\sigma \qquad (13)$$

Equation (13) is the second order differential equation which describes R.H.P. of boehmite. Since boehmite goes through a phase transformation between room temperature and 600°C it is likely that the constants H, T, R, and D will be functions of temperature. Moreover, these constants may be also functions of pressure. It would be simpler if the constants were found to be pressure independent. Then, for a given temperature if H, T, R, and D are known, the compaction curve for boehmite could be calculated for any pressure. The next step is to develop a model from which H, T, R, and D can be related to mechanical parameters.

4.3 The Mechanical Analog

A mechanical model based on linear devices like springs and dashpots can be developed, in which the constants H, T, R, and D can be expressed in terms of these devices. A spring being an ideal device for which the stress is directly proportional to the strain, while a dashpot is a hypothetical device which is strain rate sensitive only (Figure 18).

At a later stage in the development of a viscoelastic model for R.H.P. of boehmite an electrical analog rather than a mechanical analog will be used, since it is less cumbersome to work in terms of electrical components rather than mechanical components. It is relatively easy to convert from one system to the other using the following rules:

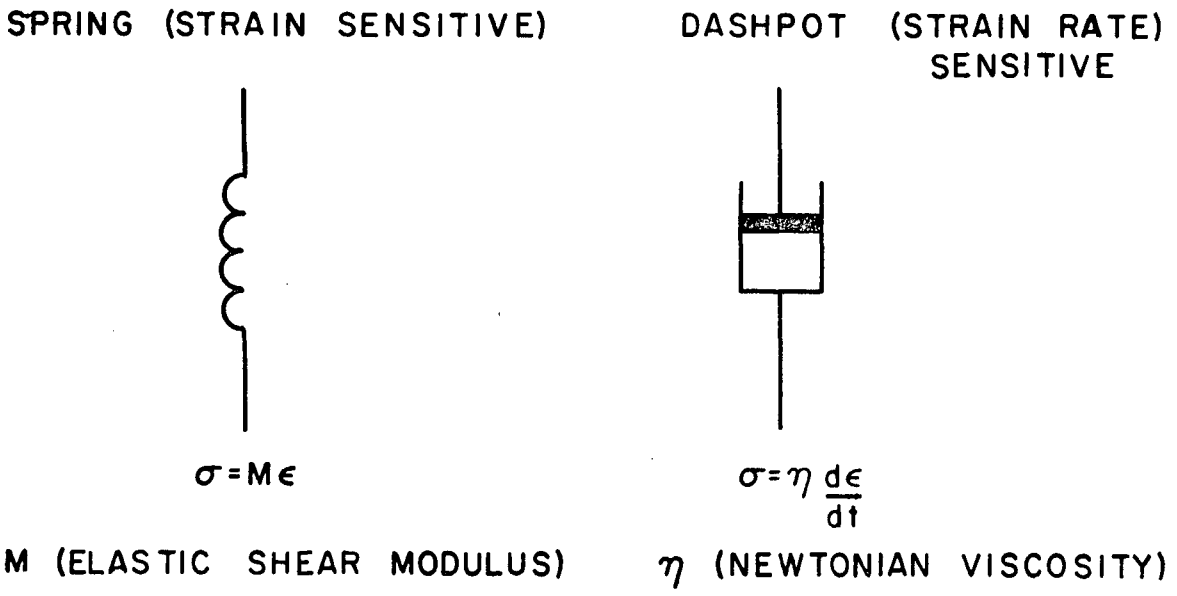

Figure 18. Defining the spring (a strain sensitive device) and dashpot (a strain rate sensitive device).

(a) Mechanical models represented by a viscoelastic theory may be converted to the electrical analog by replacing springs by capacitors, dashpots by resistors, and by changing parallel coupling to series and series to parallel (18).

(b) Using the following table (19).

MECHANICAL			ELECTRICAL	
spring	component	(1/M)	capacitor	(C)
dashpot		(η)	resistor	(R)
stress		(σ)	voltage	(v)
strain		(ε)	charge	(q)

Table V. Conversion from electrical to mechanical analog.

To demonstrate that the electrical and mechanical analogs are equivalent, both giving the same answer, the equation of motion for one of the simplest viscoelastic systems, the Voigt or Kelvin element has been calculated using both methods. These calculations are shown in Appendix B.

4.4 The Viscoelastic Model for R.H.P. of Boehmite

It has been shown in Section 4.2 that the dynamics for R.H.P. of boehmite can be expressed by a second order linear differential equation of the form

$$\frac{d\varepsilon^2}{dt^2} + H\frac{d\varepsilon}{dt} + T\varepsilon = R\frac{d\sigma}{dt} + D\sigma \qquad (14)$$

Where ε = strain

σ = stress

H, T, R, and D are constants*

with the corresponding transfer function

$$X = \frac{RS + D}{S^2 + HS + T} \qquad (15)$$

The next step is to derive an electrical analog from which the mechanical equivalent can be determined. The constants H, T, R, and D can then

---

* For constant temperature and pressure.

be expressed in terms of spring (M) and dashpot (η) parameters.

Replacing $\varepsilon \rightarrow q$ and $\sigma \rightarrow v$ (Section 4.3)

and by definition $i = \frac{dq}{dt}$

Equation 14 can be rewritten as

$$\frac{di}{dt} + Hi + T\int i\,dt = \frac{R\,dv}{dt} + Dv$$

taking the derivative

$$\frac{d^2i}{dt^2} + H\frac{di}{dt} + Ti = R\frac{d^2v}{dt^2} + D\frac{dv}{dt}$$

for which the Laplace transform is

$$S^2I + HSI + TI = RS^2V + DSV \ ^{\dagger}$$

or $$\frac{I}{V} = \frac{S[RS+D]}{S^2+HS+T} \qquad (16)$$

Therefore, the electrical analog which is required must have a transfer function of the form (16).

At this juncture one considers various combinations of resistors and condensors and calculates the transfer function for each combination.

---

† Capital letters are being used for the Laplace transformation.

The combination which has the same transfer function as equation (16) is the combination required. The simplest arrangement of resistors and condensors found to have the correct transfer function is shown in Figure 19.

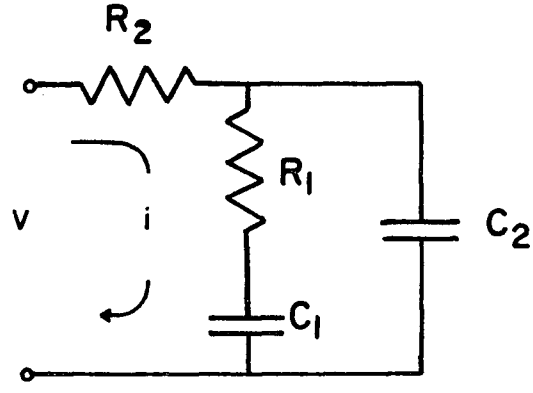

Figure 19. Electrical analog.

Since $\frac{V}{I} = Z = R_2 + \sqcup\!\sqcup$ (17)

where $\frac{1}{\sqcup\!\sqcup} = SC_2 + \frac{1}{R_1 + \frac{1}{C_1 S}} = SC_2 + \frac{C_1 S}{R_1 C_1 S + 1}$

$$= \frac{R_1 C_1 C_2 S^2 + (C_1 + C_2)S}{R_1 C_1 S + 1}$$

substituting for $\sqcup\!\sqcup$

$$Z = \frac{(R_1 R_2 C_1 C_2)S^2 + [R_2(C_1 + C_2) + R_1 C_1]S + 1}{(R_1 C_1 C_2)S^2 + (C_1 + C_2)S}$$

or

$$\frac{I}{V} = \frac{1}{Z} = \frac{(R_1C_1C_2)S^2 + (C_1 + C_2)S}{(R_1R_2C_1C_2)S^2 + [R_2(C_1 + C_2) + R_1C_1]S + 1}$$

dividing the denominator and numerator by $R_1R_2C_1C_2$

$$\frac{I}{V} = \frac{\left[\frac{1}{R_2}\right] S^2 + \left[\frac{C_1 + C_2}{R_1R_2C_1C_2}\right] S}{S^2 + \left[\frac{R_2(C_1 + C_2) + R_1C_1}{R_1R_2C_1C_2}\right] S + \frac{1}{R_1R_2C_1C_2}} \qquad (18)$$

which is the form required.

Now $i = \frac{dq}{dt}$ or $I = \mathcal{L}[i] = SQ$

therefore $\frac{I}{V} = \frac{SQ}{V}$

Substituting

$$\frac{Q}{V} = \frac{\left[\frac{1}{R_2}\right] S + \frac{C_1 + C_2}{R_1R_2C_1C_2}}{S^2 + \left[\frac{R_2(C_1 + C_2) + R_1C_1}{R_1R_2C_1C_2}\right] S + \frac{1}{R_1R_2C_1C_2}} \qquad (19)$$

The electrical analog can now be converted to the mechanical equivalent by applying the rules given in Section 4.3 or

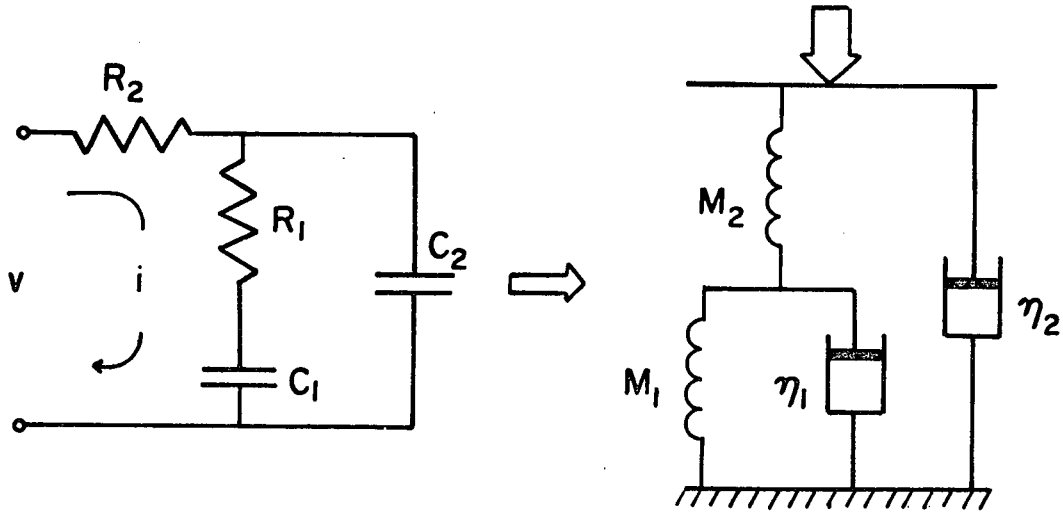

Figure 20. Electrical to mechanical analog.

and replacing $R \rightarrow \eta$

$C \rightarrow 1/M$

$q \rightarrow \varepsilon$

$v \rightarrow \sigma$

equation (19) becomes

$$\frac{E}{\square} = \left[\frac{1}{\eta_2}\right] S + \left[\frac{1/M_1 + 1/M_2}{\frac{\eta_1\eta_2}{M_1M_2}}\right] \Big/ S^2 + \left[\frac{\eta_2\left(\frac{1}{M_1} + \frac{1}{M_2}\right) + \frac{\eta_1}{M_1}}{\frac{\eta_1\eta_2}{M_1M_2}}\right] S +$$

$$\left[\frac{M_1M_2}{\eta_1\eta_2}\right] \quad (20)$$

or expressing as a differential equation and rearranging the coefficients

$$\frac{d^2\varepsilon}{dt^2} + \left[\frac{\eta_2(M_1 + M_2) + M_2\eta_1}{\eta_1\eta_2}\right]\frac{d\varepsilon}{dt} + \left[\frac{M_1M_2}{\eta_1\eta_2}\right]\varepsilon = \left[\frac{1}{\eta_2}\right]\frac{d\sigma}{dt} + \left[\frac{M_1 + M_2}{\eta_1\eta_2}\right]\sigma \qquad (21)$$

Equation (21) can now be compared with the original reactive hot pressing equation

$$\frac{d\varepsilon^2}{dt^2} + H\frac{d\varepsilon}{dt} + T\varepsilon = R\frac{d\sigma}{dt} + D\sigma \qquad (13)$$

therefore one obtains

$$H = \frac{M_1 + M_2}{\eta_1} + \frac{M_2}{\eta_2} \qquad (22a)$$

$$T = \frac{M_1M_2}{\eta_1\eta_2} \qquad (22b)$$

$$R = 1/\eta_2 \qquad (22c)$$

$$D = (M_1 + M_2)/\eta_1\eta_2 \qquad (22d)$$

but from Section 4.2

$$R = K[A\alpha + B\beta]$$

$$D = K\alpha\beta$$

$$H = \alpha+\beta$$

$$T = \alpha\beta$$

it follows

$$\eta_2 = \frac{1}{K[A\alpha + B\beta]} \tag{23a}$$

$$M_2 = \eta_2[H - D\eta_2] \tag{23b}$$

$$\eta_1 = \frac{M_2^2}{\eta_2[DM_2 - T]} \tag{23c}$$

$$M_1 = \frac{\eta_1\eta_2 T}{M_2} \tag{23d}$$

As a result of the analyses carried out in the preceding section, the mechanical model which satisfied the R.H.P. conditions is shown in Figure 21.

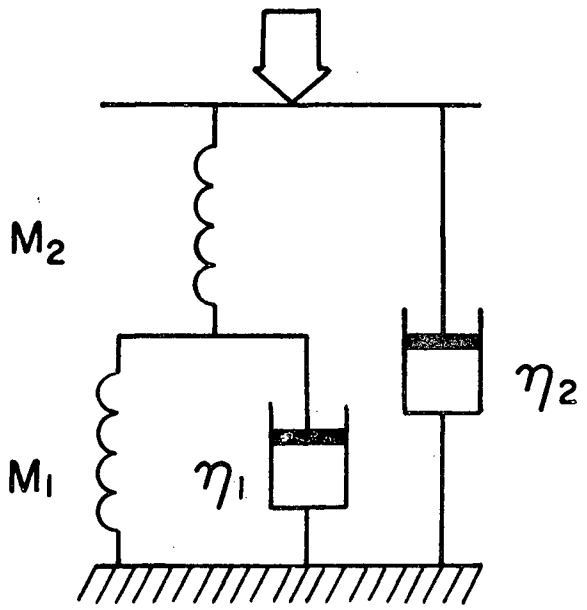

Figure 21. The mechanical analog for R.H.P. of boehmite.

The parameters η_1, η_2, M_1 and M_2 can now be calculated from K, α, A, β, and B.

4.5 Calculation of Compaction Curves for Different Pressures at Constant Temperature

If the coefficients in the differential equation are independent of pressure, then knowing R, D, T, and H for a given temperature, it should be possible to calculate the compaction curve at different pressures, assuming the same temperature is maintained. For example, boehmite was R.H.P. at 498°C and 5860 psi and the experimental data gives an excellent fit to the equation [see Figure 14a].

$$\varepsilon = \frac{\Delta L}{L_o} = (0.112)(1 - 0.472e^{-0.19t} - 0.528e^{-2.87t}) \qquad (24)$$

The compaction curve for 498°C and 9170 psi can be calculated by substituting "σ" into equation (13) where

$$\sigma = \frac{\sigma_{applied}}{\sigma_{ref}} U_{-1}(t) = \frac{9170}{5860} U_{-1}(t) = 1.56\ U_{-1}(t)$$

In general letting $\frac{\sigma_{applied}}{\sigma_{ref}} = M$, it can be shown (Appendix A) that the compaction curve at any pressure can be expressed by

$$\varepsilon = MK[1 - Ae^{-\alpha t} - Be^{-\beta t}] \qquad (25)$$

Effectively, this means that the total compaction at time equal to infinity is directly proportional to the applied pressure (stress) or

$$\frac{\left[\frac{\Delta L}{L_o}\right]_{\substack{t=\infty \\ \sigma=\text{applied}}}}{\left[\frac{\Delta L}{L_o}\right]_{\substack{t=\infty \\ \sigma=\text{ref}}}} = \frac{MK}{K} = M = \frac{\sigma_{\text{applied}}}{\sigma_{\text{ref}}} \tag{26}$$

It is unlikely that such a simple relationship is going to hold, especially at higher pressures. Previous investigation on the cold compaction behaviour of oxides by Cooper and Eaton (20) showed that the fractional volume compaction V^* can be expressed as

$$V^* = \frac{V_o - V}{V_o - V_\infty} = a_1 e^{-K_1/\sigma} + a_2 e^{-K_2/\sigma} = \frac{L_o - L}{L_o - L_\infty} \tag{27}$$

where

a_1, a_2, K_1 and K_2 are constants

V_o = initial volume ("L" initial length)

V = final volume at pressure σ

V_∞ = volume at theoretical density.

Therefore

$$\frac{\left[\frac{\Delta L}{L_o}\right]_{App}}{\left[\frac{\Delta L}{L_o}\right]_{Ref}} = \frac{a_1 e^{-K_1/\sigma_a} + a_2 e^{-K_2/\sigma_a}}{a_1 e^{-K_1/\sigma_R} + a_2 e^{-K_2/\sigma_R}} \tag{28}$$

By using Table VI in which Cooper and Eaton have summarized values of a_i and K_i for four different materials, one can obtain some idea of how much error would be introduced if equation (26) is used.

Material	K_1(psi)	K_2(psi)	a_1	a_1+a_2
Alumina	3100	50,000	0.50	0.85
Silica	2400	54,000	0.60	0.85
Magnesia	2400	49,000	0.65	0.90
Calcite	1450	42,000	0.68	1.00

Table VI. Summarized values of coefficients a_i and K_i for each powder.

For example, for alpha alumina, using an applied pressure of 6000 psi and comparing to a reference pressure of 3000 psi, equation (26) gives M = 2, while equation (28) gives M = 1.68. Therefore, by assuming that the final compaction was proportional to the applied stress for alpha alumina would have led to 16% error. Equation (25) can therefore be written in a more exact form by substituting equation (28) for "M" or

$$\varepsilon = K \left[\frac{a_1 e^{-K_1/\sigma_a} + a_2 e^{-K_2/\sigma_a}}{a_1 e^{-K_2/\sigma_R} + a_2 e^{-K_2/\sigma_R}} \right] (1-Ae^{-\alpha t} - Be^{-\beta t}) \qquad (29)$$

This is a very complicated expression, where the constants a_1, a_2, K_1 and K_2 would have to be evaluated experimentally, using the same procedures as used by Cooper and Eaton. Fortunately for the R.H.P. of boehmite and for the range of applied pressures used, the assumption that the total compaction is proportional to the applied stress gave reasonable agreement with experimental observations, as shown in Figure 27. Using the expression $M = \frac{\sigma_{App}}{\sigma_{Ref}}$ thus proved to be a good approximation.

4.6 Calculation of η_1, M_1, η_2 and M_2

In Table VII the values of K, A, α, B and β are summarized, for each compaction curve shown in Figure 13. From this information and using equations (23a-d) the value of η_1, M_1, η_2 and M_2 can be calculated for each curve. The final results are graphically shown in Figure 22, where these parameters are plotted as a function of temperature.

Figure 22 allows one to visualize the entire R.H.P. behaviour of boehmite as a function of temperature. More important the viscous and elastic nature of boehmite during R.H.P. can be easily distinguished. The elastic component M_2 and the viscous component η_2 are small compared to M_1 and η_1, and are nearly temperature independent. For this reason both M_2 and η_2 can be assumed to be negligible. The R.H.P. model for boehmite thus can be approximated by a simple Voigt or Kelvin visco-elastic element (Figure 23) which assumes that any changes in the strain of the elastic component are viscously damped. The effect of temperature on the viscous component η_1 and the elastic component M_1

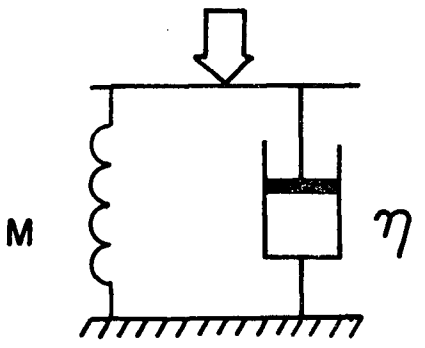

Figure 23. Voigt or Kelvin viscoelastic element.

Run No.	Temp. °C	K $[\frac{\Delta L}{L_o}]$	A	α	B	β	Density ρ	Elastic comp. M_1	Viscous comp. η_1	Elastic comp. M_2	Viscous comp. η_2	$M_T = \frac{M_1 M_2}{M_1+M_2}$	$1/M_T$
33	270	0.126	0.319	250	.681	4.81	1.42	28	108	11	2	7.9	.127
30	290	0.144	.218	.262	.782	2.66	1.47	39	146	8	3	6.7	.149
22	400	0.099	.249	.302	.751	2.98	1.41	50	162	13	4	10.3	.097
26	420	0.080	.368	.093	.632	2.1	1.37	37	391	19	9	12.5	.080
27	498	0.112	.422	.190	.528	2.87	1.45	22	108	15	6	8.9	.112
29	529	0.120	.511	.314	.489	2.91	1.49	21	60	14	5	8.4	.119
15	540	0.121	.525	.236	.475	1.99	-	20.6	78	14	8	8.3	.120
23	622	0.135	.259	.260	.741	2.81	-	35	130	9	3	7.2	.139
28	628	0.103	.188	.405	.812	4.34	1.42	63	152	11	3	9.4	.106

Table VII. Summary of viscoelastic components.

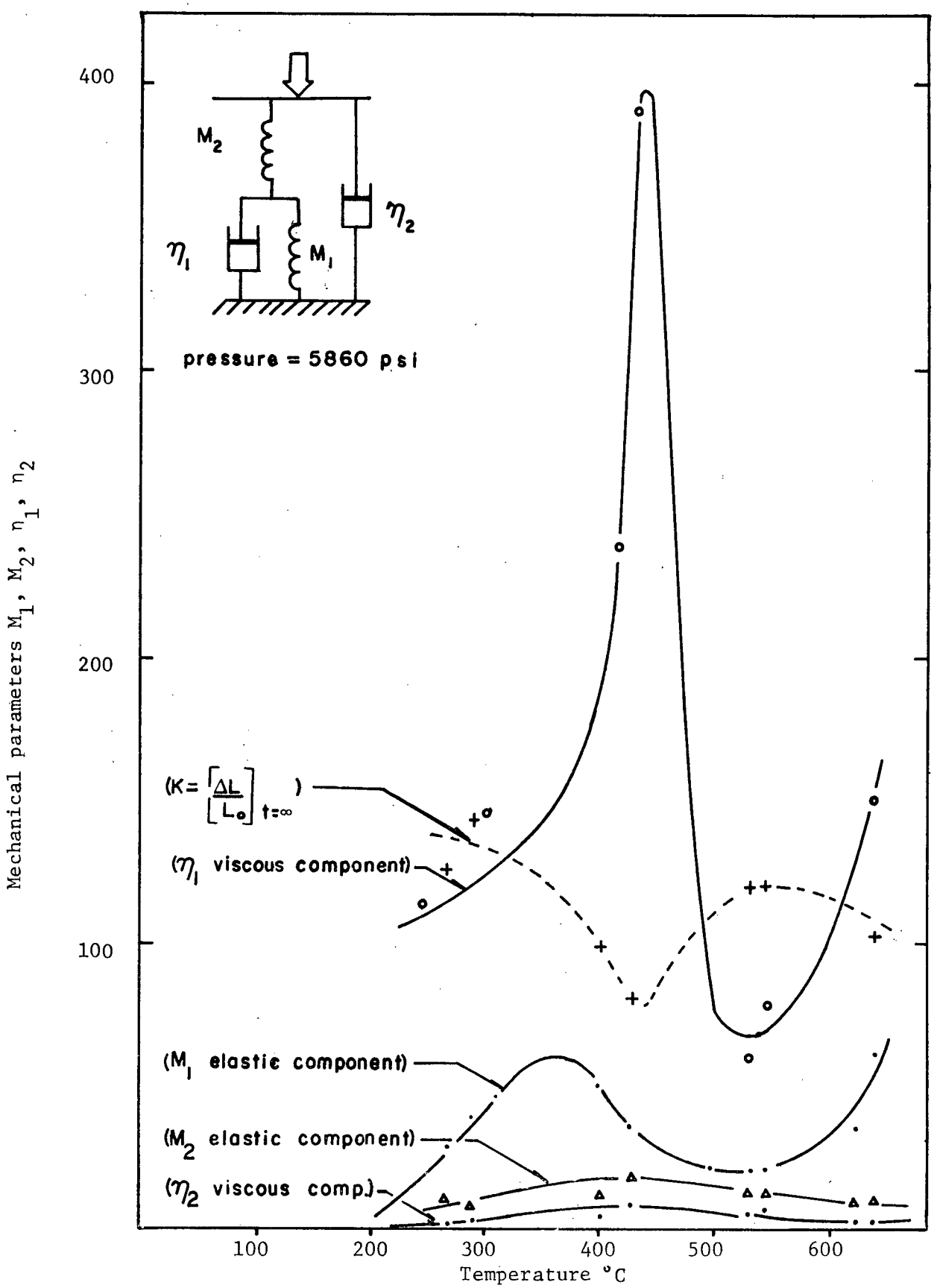

Figure 22. Mechanical parameters versus temperature.

is very drastic. In fact, there is excellent correlation between the behaviour of η_1 and the D.T.A. for boehmite (see Figure 24).

The R.H.P. behaviour of boehmite as a function of temperature will be discussed in four stages.

4.6.1 Stage (a) - R.T. to 275°C

Referring to both the D.T.A. (Figure 25) and the T.G.A. (Figure 26) one can see a large endothermic peak at 107°C corresponding to the impurities (acetate and $SO_4^{=}$) being driven off. In stage (a) approximately 0.10 H_2O molecules per Al_2O_3 molecule is lost due to dehydroxylation. At 275°C, the D.T.A. shows a baseline peak. This corresponds to a change in the rate of dehydroxylation and the start of stage (b).

4.6.2 Stage (b) - 275°C to 443°C

Stage (b) has been divided into two sub-regions, region I and the viscous region II. At 275°C both the elastic component M_1 and the viscous component η_1 are comparatively small (Figure 22). However, as the temperature is increased both M_1 and η_1 start to increase. The elastic component M_1 reached its peak value at approximately 380°C. This is the beginning of the viscous region II.

(i) The viscous region 380°C to 443°C

The viscous region is introduced with no apparent change in the rate of dehydration (Figure 26), however, at this temperature approximately 0.5 H_2O molecules of water have been removed due to dehydration. Noting that the original Dupont Baymal colloidal allumina

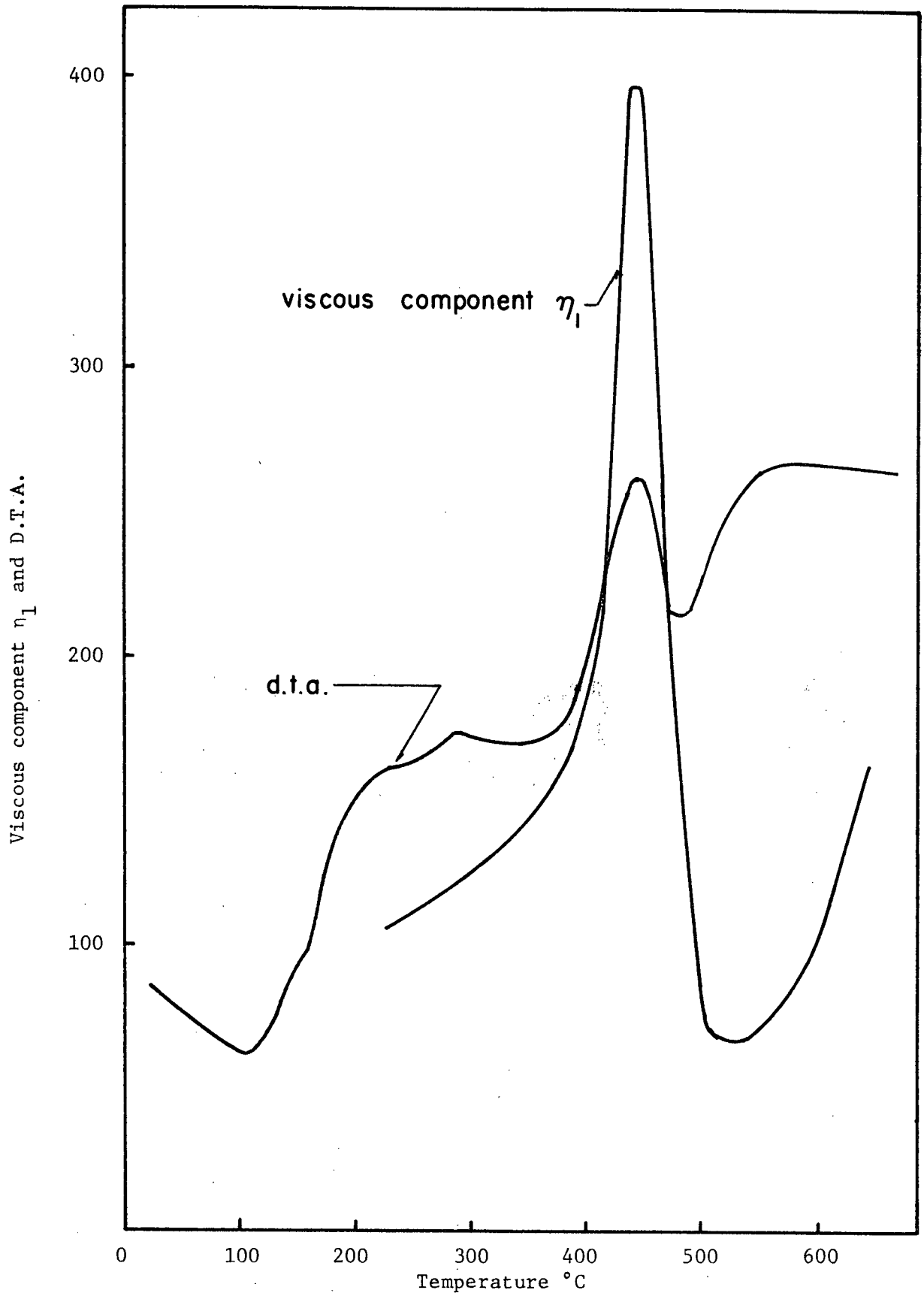

Figure 24. Comparison of the D.T.A. curve and the viscous component η_1.

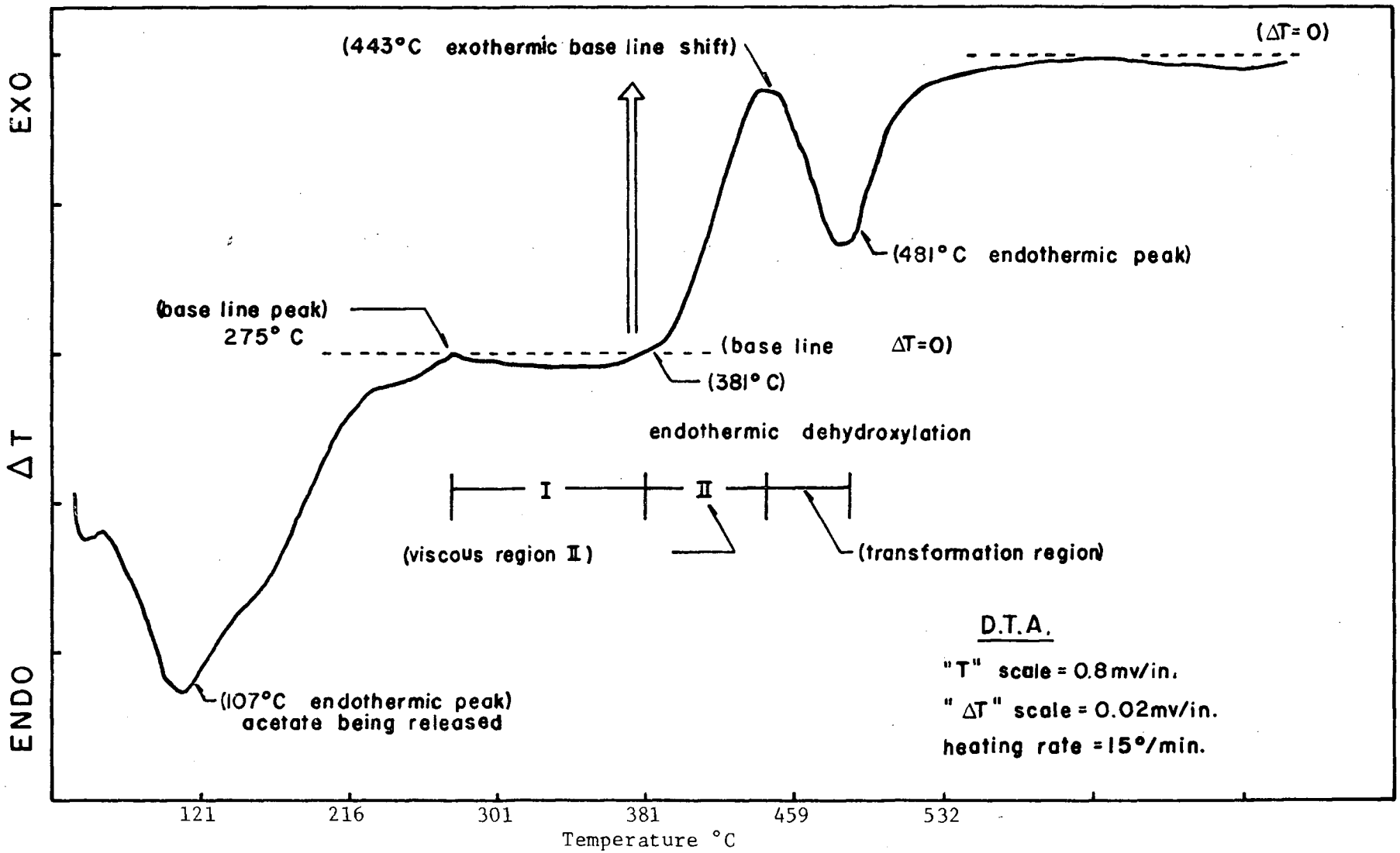

Figure 25. D.T.A. for boehmite (plat. versus plat. +13% rhodium thermocouple).

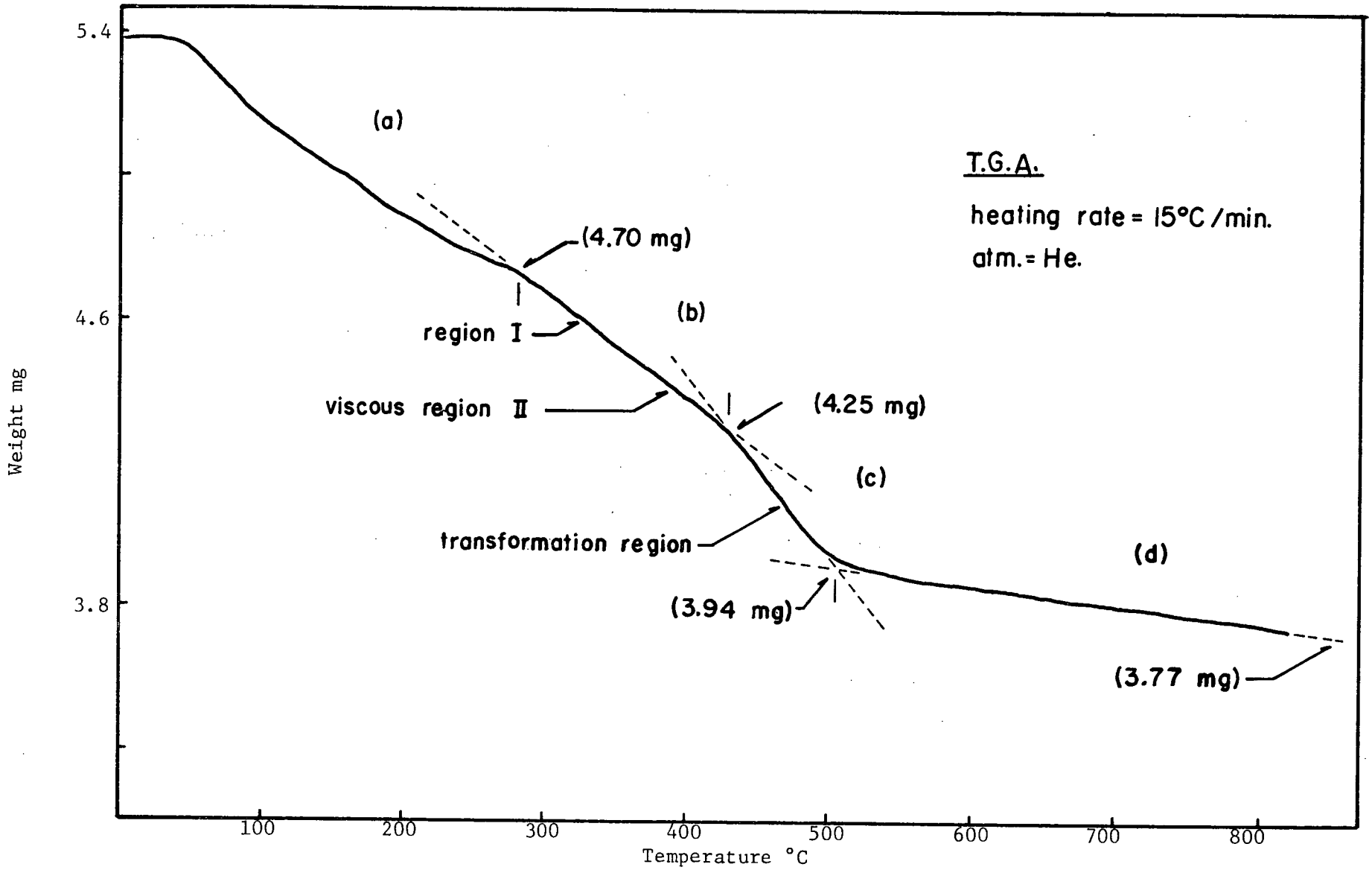

Figure 26. T.G.A. for boehmite.

(boehmite) consisted of $Al_2O_3.1.5H_2O$ or 0.5 H_2O molecules/Al_2O_3 must have existed as physically absorbed water.*

At 380°C all the physically absorbed water has been driven off. What is left is $Al_2O_3.H_2O$, the empirical formula usually given for boehmite. Therefore,it is expected that any further removal of water will result in free surface bond formation or active sites. This is verified by the increase in viscosity, shown in Figure 22. For temperatures above 380°C the viscous component increases drastically, peaking at 443°C, while there is a corresponding exothermic base shift on the D.T.A. curve. The viscous nature of the boehmite supports the idea of a very active surface (large surface free energy) above 380°C. The small fibrillar boehmite particles will coalesce together, the shear force for interparticle sliding will increase. This is equivalent to sintering. However, sintering suggests particle volume changes to compensate for neck growth. It is possible that in this case, however, the particles stick together not unlike two oppositely charged sheets of paper rather than sintering with associated volume change. It has been suggested, that surface melting may be taking place, but surface melting would be an endothermic reaction. Also, if the surface consists of only a few monolayers then it is meaningless to talk about a liquid zone. On the other hand,it should be possible to detect large amounts of melting in this region by X-ray methods (particle size determination).

* According to Tertian and Papee, excess water represented by $Al_2O_3.1.6H_2O$ if retained as a monolayer would cover about $265m^2/g$, essentially the total active surface of pseudoboehmite. The surface area for Baymal colloidal alumina is 250 m^2/g.

From the D.T.A. Curve it can be seen that the onset of the viscous region is associated with a large exothermic base shift. It is unlikely that recrystallization between particles could account for such a large ΔT change. More likely, the change is due to a change in the effective thermal conductivity of the material (7), which would result from sintering. It is interesting to note, that the D.T.A. was repeated at different rates of heating 15°C/min and 3°C/min. The shape of the D.T.A. curve did not change throughout the viscous region. This suggests that coalescence of the particles must take place very quickly, the degree of coalescence being proportional to the temperature; as the temperature is increased more water is driven off resulting in a greater number of active sites.

(ii) The viscous region and "steady state"

Referring to Figure 13, it is noticed that for the experiment carried out at 400°C (run 27), the compaction behaviour approaches a steady state during the latter stages. The corresponding compaction rate is 1.1×10^{-3}/min. This is indicative of the predominant viscous nature of the powder at this temperature. A simple attempt can be made as follows to predict the slope of the "steady state" curve for any temperature (380 to 443°C) within the viscous region using the results from the D.T.A. Comparing both the D.T.A. and the viscous component η_1, one will immediately see that they behave in a similar manner. Generalizing one can write

$$\eta \propto \frac{\Delta T}{T} \qquad \text{or } \eta = K' \frac{\Delta T}{T}$$

But $\sigma = \eta \frac{d\varepsilon}{dt}$ (by definition)

Substituting $\frac{d\varepsilon}{dt} = \frac{K''}{\frac{\Delta T}{T}}$

However, in the viscous region from the D.T.A. $dT = \xi T + \gamma$

Therefore $\frac{d\varepsilon}{dt} = \frac{K''}{\xi + \frac{\gamma}{T}}$ where K", ξ and γ are constants.

That is, the strain rate is temperature sensitive only.

4.6.3 Stage (c) - Transformation Region 443°C to 520°C

From 443°C to 520°C both the viscous component η_1 and the elastic component M_1 decrease to a minimum. This is the temperature at which boehmite transforms to gamma alumina. The transformation is accompanied by the largest rate of dehydroxylation. At 520°C, the start of stage "d", if it is assumed that boehmite has been completely converted to gamma alumina, then gamma alumina still contains approximately 4% water.

4.7 The Effect of Pressure on R.H.P. of Boehmite

To test the theory at a different pressure, boehmite was hot pressed at 9170 psi and 513°C. In theory one could obtain M_1, M_2, η_1 and η_2 at 513°C and 5860 psi from Figure 22, then calculate α, β, A and B. From this data the compaction behaviour at 9170 psi could be calculated using the theory in Section 4.5. Since it was difficult experimentally to achieve the same temperature between different runs, the average values from run 29 at 529°C and run 27 at 498°C were used (see Table VIII).

	Run 29 at 529°C (5860 psi)	Run 27 at 498°C (5860 psi)	Average
K	0.120	0.112	0.116
A	0.511	0.472	0.491
α	0.314	0.190	0.252
B	0.489	0.528	0.508
β	2.91	2.87	2.89
M_1	20.7	21.8	21.7
M_2	13.8	15.1	14.4
η_1	60.1	108.6	84.3
η_2	5.26	5.56	5.41

Table VIII. Average values for mechanical parameters at 513°C.

From the theory, the compaction curve for 9170 psi is given by

$$\varepsilon = MK\{1-Ae^{-\alpha t} - Be^{-\beta t}\} \tag{25}$$

where

$$M = \frac{\sigma_{App}}{\sigma_{Ref}} = \frac{9170}{5860} = 1.56 \tag{30}$$

therefore at 9170 psi and 513°C

$$\varepsilon = (0.182)(1 - 0.491e^{-0.252t} - 0.508e^{-2.89t}) \tag{31}$$

$\varepsilon = \frac{\Delta L}{L_o}$ is plotted in Figure 27 along with the experimental R.H.P. curve at 9170 psi. The agreement between the two is reasonable. Also, it justifies using the simple assumption that the final compaction is

proportional to the applied stress. It should be realized that under the experimental conditions used, the final compact densities were always less than 75% theoretical density (based on the theoretical density of gamma alumina).

4.8 The Viscoelastic Model and Apparent End-Point Density

One of the most difficult parameters to measure accurately is the total compaction "K". During R.H.P. one must initially start with a green compact, therefore, it is imperative that the density of the green compact be carefully controlled. Any variations in green density between specimens would result in a measureable error in "K". St-Jacques solved this problem by prepacking at a constant rate using an Instron machine. However, for the present work it was technically impossible to achieve such control. For this reason, the results as shown in Figure 22 are only qualitative in nature, but accurate enough to show the general trend in the behaviour of boehmite during reactive hot pressing. The degree of accuracy can be checked by measuring the final compact density. The end-point density* (under stress) for a compact should be inversely proportional to the total elastic component. From Figure 22 the total elastic component is just two springs, of elastic constant M_1 and M_2 in series. This is equivalent to a single spring with effective elastic constant $M_T = \frac{M_1 M_2}{M_1+M_2}$. $1/M_T$ has been plotted as a function of temperature, along with the apparent end-point density in Figure 28. These two curves

* Note, the end-point density (under stress) is approximately equal to the final compact density (see Figure 2, a schematic diagram of a typical R.H.P. cycle). The spring back on cooling is less than 0.005 inches.

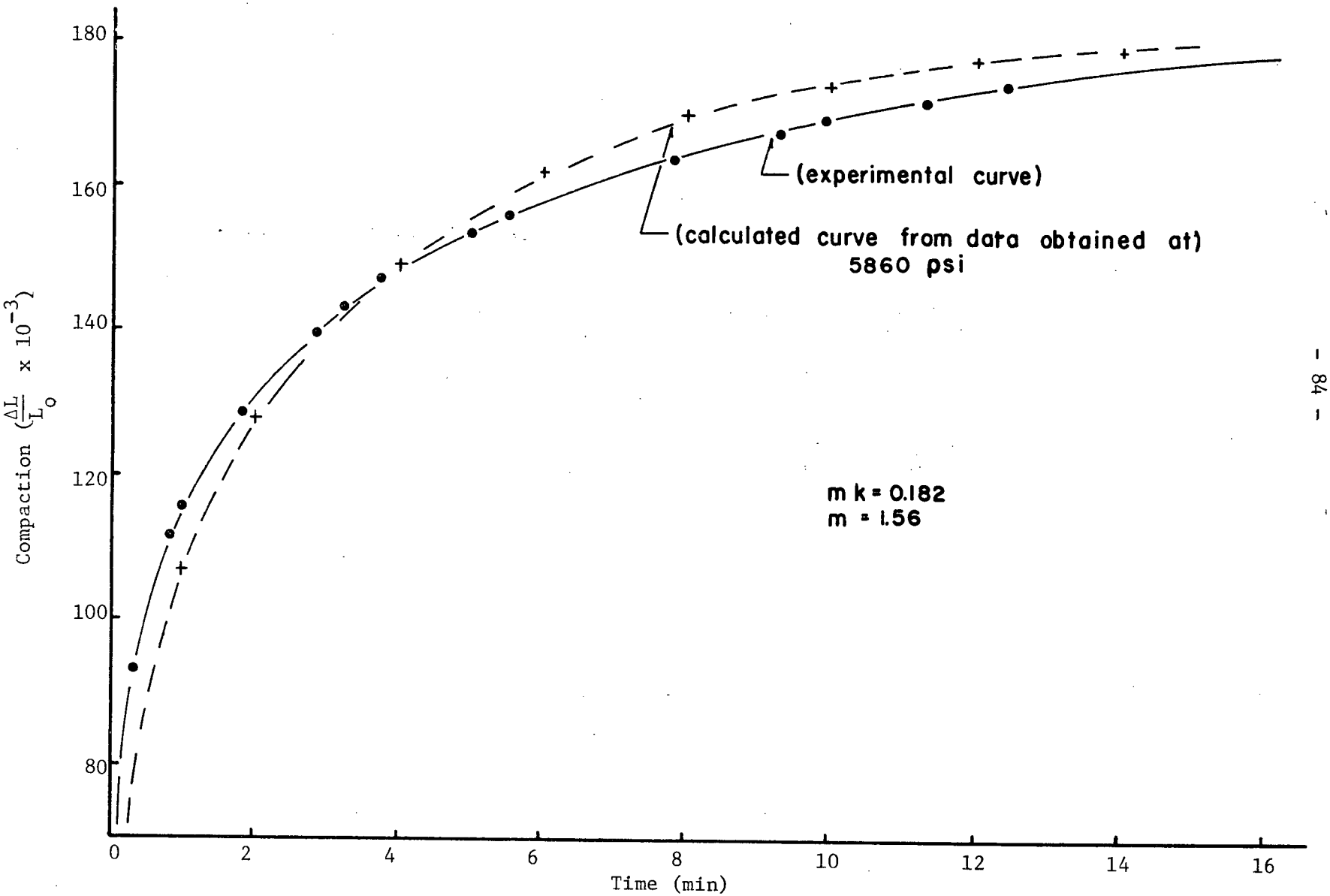

Figure 27. Compaction curve for boehmite at 513°C and 9170 psi.

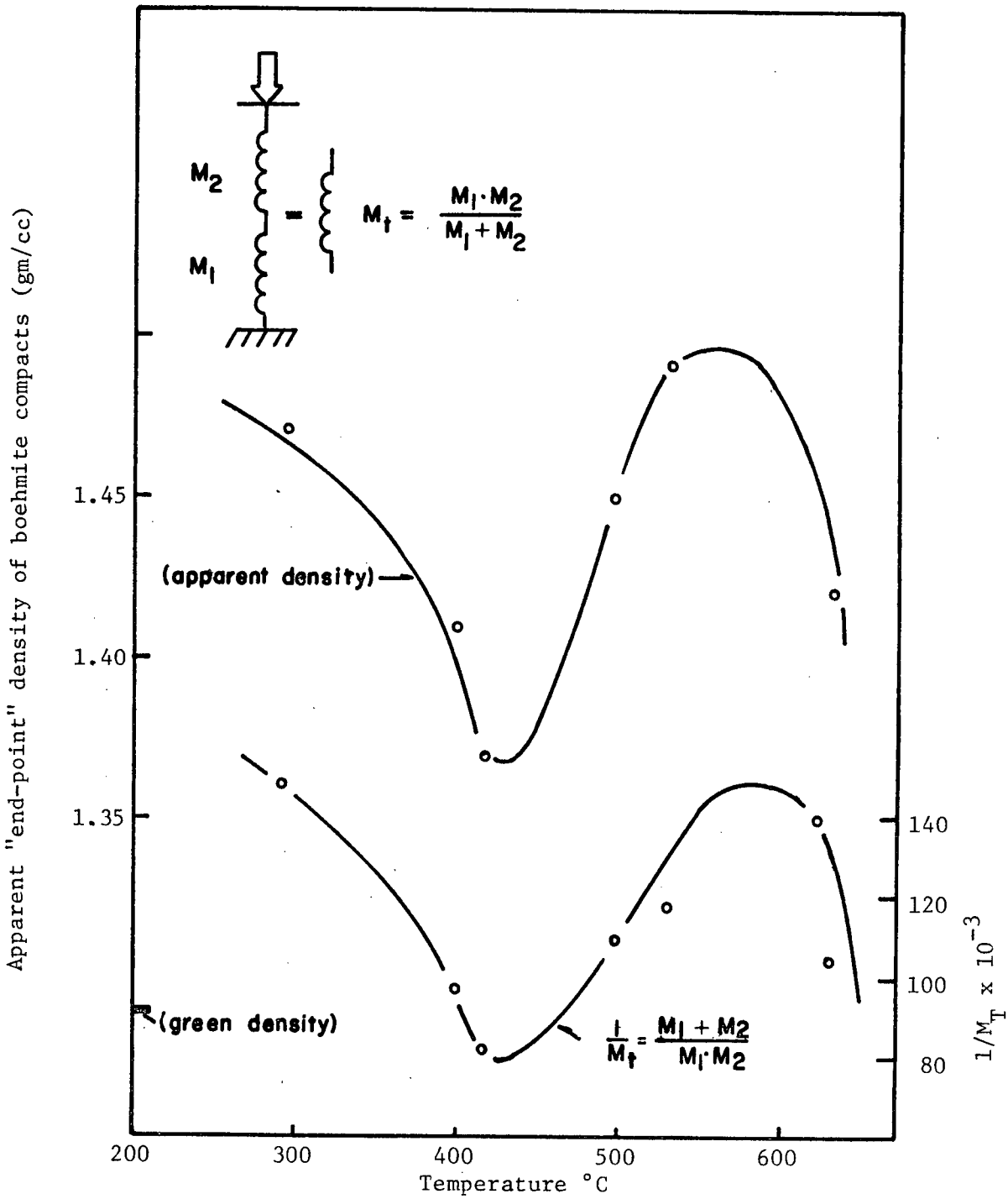

Figure 28. A comparison of apparent "end-point" density to total elastic constant M_T

are similar, demonstrating that apparent density is approximately inversely proportional to M_T. Also, this calculation checks the self-consistency of the viscoelastic model used in the interpretation of the hot-pressing data.

CONCLUSION

1. It has been possible to produce a hard dense phase (2.2 gm/cc) by reactive hot pressing fibrillar boehmite during its transformation to gamma alumina at 500°C. Formation of the "hard phase" material however, depended on achieving and maintaining the correct vapor pressure during the R.H.P. operation. At least 4% retained water must be maintained in order for the "hard phase" to form. On the other hand, if the vapor pressure was allowed to become too high(because of gas trapped within the die assembly during R.H.P.), the boehmite powder appears to transform directly to alpha alumina. Under these conditions, it is impossible to produce a dense strong compact at 500°C.

2. The isothermal compaction data was analysed using a viscoelastic model. It was possible to correlate adequately experimental data obtained from the D.T.A. and T.G.A. to the behaviour of boehmite during hot pressing by this model. Although the isothermal behaviour of boehmite was a complex function of temperature it was possible to arrive at the following conclusions:

(i) The final compaction was not proportional to the total weight loss, contrary to the findings of Cook.

(ii) The total compaction at a given temperature was proportional to the applied stress within the range of applied pressures used in this study (9200 psi max.).

(iii) Within the temperature range 380 to 443°C the powder was found to behave in a viscous fashion, suggesting particle interaction

was taking place. It is expected that reactive hot pressing at any temperature within this range should produce the most favourable particle alignment for converting a powder compact into the hard dense material at 500°C.

(iv) During the viscous deformation the strain rate (to a first approximation) was found to be temperature sensitive only, indicating pseudo-Newtonian behaviour.

3. Production of the hard phase material at 500°C seems promising as an intermediate step in producing strong sintered alumina products at low temperatures. Although previously not mentioned, it was found that if the "hard phase" material is sintered at 1000°C ($< T_{m/2}$) for 6 hours it is possible to produce a hard, strong and translucent body.

APPENDIX A

The compaction curve for $\sigma_{Applied} \neq \sigma_{Ref}$ can be calculated by expanding equation (6) by partials, or

$$E = X\square = \frac{MRS + MD}{S(S^2+HS+T)} = \frac{MRS + MD}{S(S+\alpha)(S+\beta)} \qquad (6)$$

since $\square = \mathcal{L}\{Mu_{-1}(t)\} = M/S$

equating equal powers of S gives

$$0 = q + f + w$$

$$MR = qH + \beta f + w\alpha$$

$$MD = Tq$$

or

$$q = MK$$

$$w = -MKB$$

$$f = -MKA$$

Therefore

$$E = \frac{MK}{S} - \frac{MKA}{S+\alpha} - \frac{MKB}{S+\beta}$$

or

$$\varepsilon = \mathcal{L}^{-1}(E) = MK\{1-Ae^{-\alpha t} - Be^{-\beta t}\} \qquad (25)$$

APPENDIX B

Comparison of the Two Methods

To demonstrate how a viscoelastic system can be calculated using either a mechanical or an electrical approach, the following system will be considered. One of the simplest viscoelastic systems is the Voigt or Kelvin element. It assumes that any changes in the strain of the elastic component are viscously damped and can be modelled as a parallel combination of springs and dashpots (18) (Figure 23).

where $\sigma_T = \sigma_E + \sigma_V$ (stress)

for the spring $\sigma_E = M\varepsilon_E$ M (elastic shear modulus)

for the dashpot $\sigma_V = \eta\frac{d\varepsilon}{dt}$ η (Newtonian viscosity)

Now $\sigma_T = \sigma_E + \sigma_V$

Substituting

$$\sigma_T = M\varepsilon_E + \eta\dot{\varepsilon}_V \qquad \text{Note } \dot{\varepsilon}_V = \frac{d\varepsilon_V}{dt}$$

But for a parallel coupling $\varepsilon_E = \varepsilon_V = \varepsilon_T$

therefore $\sigma_T = M\varepsilon_T + \eta\dot{\varepsilon}_T$ or integrating

$$\varepsilon_T = e^{-t/\tau}[\varepsilon_o + 1/\eta \int \sigma(t)e^{t/\tau}dt]$$

where ε_o = strain at time = 0

$\tau = \eta/M$

The response of the system to a constant stress is therefore

$$\sigma(t) = \sigma_o$$

$$\varepsilon_T = \frac{\sigma_o}{M} + [\varepsilon_o - \frac{\sigma_o}{M}]e^{-t/\tau} \quad (a)$$

and for the following boundary conditions, at time = 0

$\varepsilon_T = 0$, then $\varepsilon_o = 0$

equation (a) becomes

$$\varepsilon_T = \frac{\sigma_o}{M}[1-e^{-t/\tau}]$$

Now the same system will be developed using the electrical analog method, from section 4.3 rule (a)

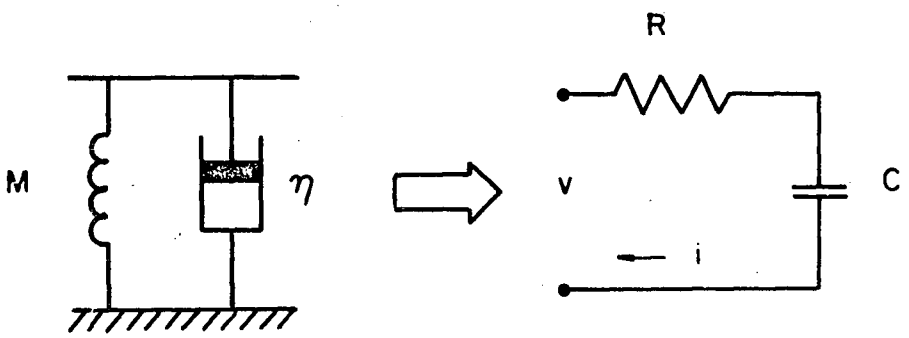

The next step is to work out the complex impedance of the electrical circuit (the complex impedance is determined by calculating the Laplacian of the ratio v to i.).

$$\text{or} \qquad Z = \frac{V}{I} = R + \frac{1}{SC} = \frac{RCS + 1}{SC}$$

Therefore $I(RCS + 1) = VSC$

The differential equation is therefore

$$RC \frac{di}{dt} + i = C \frac{dv}{dt}$$

Substituting

$$\frac{d^2q}{dt^2} + \frac{1}{RC} \frac{dq}{dt} = \frac{1}{R} \frac{dv}{dt}$$

and integrating

$$\frac{dq}{dt} + \frac{1}{RC} q = \frac{1}{R} v$$

from Table V, Section 4.3

$$q \rightarrow \varepsilon \qquad R \rightarrow \eta$$

$$v \rightarrow \sigma \qquad C \rightarrow 1/M$$

The mechanical equivalent is therefore

$$\frac{d\varepsilon}{dt} + \frac{M}{\eta}\varepsilon = \frac{1}{\eta}\sigma \qquad \text{and for } \sigma = \sigma_o \text{ (constant)}$$

The solution for this equation is

$$\varepsilon = \varepsilon_{\text{homogeneous}} + \varepsilon_{\text{steady state}}$$

Homogeneous

$$\frac{d\varepsilon_H}{dt} + \frac{M}{\eta}\varepsilon_H = 0$$

let

$$\varepsilon_H = Ae^{\alpha t}$$

substituting

$$\alpha = -M/\eta$$

therefore

$$\varepsilon_H = Ae^{-M/\eta\, t} = Ae^{-t/\tau} \qquad \text{where } \tau = \eta/M$$

Steady State Solution

$$\frac{M}{\eta}\varepsilon_{SS} = \frac{1}{\eta}\sigma_o \qquad \text{or} \qquad \varepsilon_{SS} = \frac{1}{M}\sigma_o$$

therefore

$$\varepsilon = Ae^{-t/\tau} + \frac{1}{M}\sigma_o$$

from the boundary condition $\varepsilon = 0$ at $t = 0$

$$A = -\frac{1}{M}\sigma_o$$

the solution is therefore

$$\varepsilon = \frac{1}{M}\sigma_o[1 - e^{-t/\tau}]$$

which is the same as obtained previously using a mechanical analog.

BIBLIOGRAPHY

1. J. Burke, N. Reed, V. Weiss, Ultrafine Grain Ceramics, Syracuse University Press (Lib UF 5263).

2. A.C.D. Chaklader, L.G. McKenzie, "Reactive Hot Pressing of Clays", American Ceramic Bulletin, 43, No. 12 (1964).

3. C.H. Bates, C.J. Drew, R.C. Kell, "Simplified Process for Preparing Translucent Alumina Tubes from Boehmite Powder", Transactions and Journal of the British Ceramic Society, 70, 4 (1971) page 128.

4. A.C.D. Chaklader and R.C. Cook, "Kinetics of Reactive Hot Pressing of Clays and Hydroxides", American Ceramic Bulletin, 47, No. 8 (1968) page 715.

5. R.G.St-Jacques, "Creep of Compacts of Colloidal Boehmite (AlOOH) during Dehydroxylation, Master Thesis, Department of Metallurgy, U.B.C., November (1968).

6. (a) J.W. Newsome, H.W. Heisser, A.S. Russell and H.C. Stumpf, "Alumina Properties" Tech. paper No. 10, page 46. Alcoa Research Laboratories, Pittsburgh, 1960.
(b) R. Tertian and D. Papee, J. Chem. Phys., 55, 541-53 (1958).

7. M. Deflandee, "The Crystal Structure of Diaspore", Bull. Soc. Franc. Min 55, 140-65 (1932).

8. R.K. Iler, "Fibrillar Colloidal Boehmite - Progressive Conversion to Gamma, Theta and Alpha Aluminas", J. Am. Ceramincs Soc. 44, (12), 618-24 (1961).

9. H. Achenbach, "Thermal Decomposition of Synthetic Hydrargillite", Chem. Erde 6, 307-56 (1931).

10. W. Gitzen, "Alumina as a Ceramic Material", The Am. Ceramic Soc., 1970 (page 32).

11. H. Saalfeld, "The Structures of Gibbsite and of the Intermediate Products of its Dehydration", N. 5b. Miner Abh. 95, 1-87 (1960).

12. H.P. Klug and L.E. Alexander, X-ray Diffraction Procedures, John Wiley and Sons, Inc., (1967) page 507.

13. Norelco instruction and operating manual for X-ray diffraction unit type No. 8 (2045-2046), (page 2A).

14. J.H. de Boer, G.M. Houbee, Proc. Intern. Sympos. Reactivity of Solids (Gothewberg I, 237 (1952)).

15. Dupont differential thermal analyzer (900) operators manual.

16. T.G. Carruthers, T.A. Wheat, Proc, Brit. Ceram. Soc., Transaction and Journal of the British Ceramic Society, A5253/C525, (1969).

17. Distefano, Stubberud, Williams, Feed back and Control Systems, Schaums outline series (page 101-problem 6.7).

18. A.J. Kennedy, Processes of Creep and Fatique in Metals, Oliver and Boyd page 9 [Lib. TA450].

19. J.H. Goldberg, Automatic Controls: Principles of System Dynamics, Allyn and Bacon Inc., (1964).

20. A.R. Cooper, L.E. Eaton, "Compaction Behaviour of Several Ceramic Powders", Amer. Cer. Moc. 45, No. 3, March 1962.

21. J.H. Fancy, F. Donald Bloss, X-Ray Diffraction, Southern Illinois University Press (Lib Q094).

22. L.G. MacKenzie, A.C.D. Chaklader, "Reactive Hot Pressing of Clays and Alumina", Journal of American Ceramics Society, 49, 490 (1966).